INFORMATION TO USERS

The most advanced technology has been used to photo-
graph and reproduce this manuscript from the microfilm
master. UMI films the text directly from the original or
copy submitted. Thus, some thesis and dissertation copies
are in typewriter face, while others may be from any type
of computer printer.

The quality of this reproduction is dependent upon the
quality of the copy submitted. Broken or indistinct print,
colored or poor quality illustrations and photographs,
print bleedthrough, substandard margins, and improper
alignment can adversely affect reproduction.

In the unlikely event that the author did not send UMI a
complete manuscript and there are missing pages, these
will be noted. Also, if unauthorized copyright material
had to be removed, a note will indicate the deletion.

Oversize materials (e.g., maps, drawings, charts) are re-
produced by sectioning the original, beginning at the
upper left-hand corner and continuing from left to right in
equal sections with small overlaps. Each original is also
photographed in one exposure and is included in reduced
form at the back of the book. These are also available as
one exposure on a standard 35mm slide or as a 17" x 23"
black and white photographic print for an additional
charge.

Photographs included in the original manuscript have
been reproduced xerographically in this copy. Higher
quality 6" x 9" black and white photographic prints are
available for any photographs or illustrations appearing
in this copy for an additional charge. Contact UMI directly
to order.

U·M·I

University Microfilms International
A Bell & Howell Information Company
300 North Zeeb Road. Ann Arbor, MI 48106-1346 USA
313/761-4700   800/521-0600

Upper crustal structure of southern Alaska: An interpretation of seismic refraction data from the Trans-Alaska Crustal Transect

Wolf, Lorraine W., Ph.D.

University of Alaska Fairbanks, 1989

U·M·I
300 N. Zeeb Rd.
Ann Arbor, MI 48106

UPPER CRUSTAL STRUCTURE OF SOUTHERN ALASKA: AN
INTERPRETATION OF SEISMIC REFRACTION DATA FROM THE
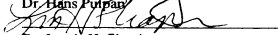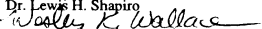TRANS-ALASKA CRUSTAL TRANSECT

by

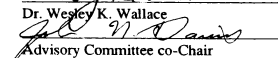Lorraine W. Wolf

RECOMMENDED:
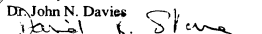
Dr. William D. Harrison

Dr. Hans Pulpan

Dr. Lewis H. Shapiro

Dr. Wesley K. Wallace
Advisory Committee co-Chair

Dr. John N. Davies
Advisory Committee co-Chair

Dr. David B. Stone
Department Head,
Geology and Geophysics

APPROVED:

Dean, College of Natural Sciences

Dean of the Graduate School

7/10/89
Date

UPPER CRUSTAL STRUCTURE OF SOUTHERN ALASKA: AN INTERPRETATION

OF SEISMIC REFRACTION DATA

FROM THE TRANS-ALASKA CRUSTAL TRANSECT

A

THESIS

Presented to the Faculty of the University of Alaska

in Partial Fulfillment of the Requirements

for the Degree of

DOCTOR OF PHILOSOPHY

By

Lorraine W. Wolf, B.A., M.A.

Fairbanks, Alaska

September 1989

ABSTRACT

Seismic refraction and wide-angle reflection data from the U.S. Geological Survey's Trans-Alaska Crustal Transect is used to investigate the upper crustal structure of southcentral Alaska. The data consist of two intersecting refraction lines: the 135-km Chugach profile which follows the E-W strike of the Chugach Mountains and the 126-km Cordova Peak profile which follows the N-S regional dip. The four shots of the Chugach profile and the five shots of the Cordova Peak profile were recorded on 120 portable seismic instruments spaced at 1-km intervals.

Interpretation of data from the Chugach terrane indicates that near-surface unconsolidated sediment and glacial ice overlie rocks of unusually high average compressional velocities (5.4-6.9 km/s) in the upper 10 km of crust. A thick unit correlated with a metasedimentary and metavolcanic flysch sequence has velocities of 5.4-5.9 km/s. It is underlain by mafic to ultramafic metavolcanic rocks (6.0-6.4 km/s) correlated with the terrane basement. Mid-crustal layers beneath the Chugach terrane contain two velocity reversals (6.5 and 6.7 km/s) attributed to off-scraped oceanic sedimentary rocks which are underlain by mafic to ultramafic oceanic volcanic crust (7.0-7.2 km/s).

Interpretation of data from the Prince William terrane indicates systematically lower velocities in Prince William terrane rocks as compared to Chugach terrane rocks

iii

at comparable depths. The upper 10 km of crust, having average compressional velocities of 3.0-6.2 km/s, is correlated with clastic sedimentary and volcanic rocks which are overlain by younger terrigenous sedimentary rocks. A 2-km thick layer at 10-12 km depth is correlated with mafic to ultramafic Prince William terrane basement rocks. The difference in velocity structure between the Chugach and Prince William terranes suggests that the Contact fault zone is a terrane boundary which extends to a depth of at least 10-12 km. Deep structure beneath the two terranes is not well constrained by the seismic refraction data. Potential field data support the interpretation that a thick low-velocity zone occurs at a 12-15 km depth and may contain subducted continental rocks of the Yakutat terrane, which is currently accreting to and being thrust beneath the North American continent along the Gulf of Alaska margin.

TABLE OF CONTENTS

v

vi

LIST OF FIGURES

vii

viii

LIST OF TABLES

ix

ACKNOWLEDGEMENTS

x

PREFACE

Southern Alaska is a geologically and tectonically complex area which offers a modern setting for the study of subduction zone environments and accretionary processes. It is a collection of tectonostratigraphic terranes which were accreted to the North American continent along the convergent North American-Pacific plate boundary (Figure 1). Each of these terranes is believed to represent a distinct, fault-bounded geologic entity with a geologic history distinct from its neighbors [Howell et al., 1985]. Numerous geologic studies have focused on the surface expression of this environment, while seismological studies have examined its deep crustal structure and dynamics. A recent contribution towards our understanding of the plate tectonic development of Alaska has come from Trans-Alaska Lithospheric Investigation (TALI) project, an ongoing program of geological studies and crustal seismic investigations which started in the Gulf of Alaska and continues northward [Stone et al., 1986].

The focus of this thesis is to increase our general understanding of the tectonic processes of plate margins, and in particular, our knowledge of the accretionary terranes of southern Alaska. In the following chapters, a three-dimensional model for a part of southern Alaska is developed from an interpretation of two intersecting

1
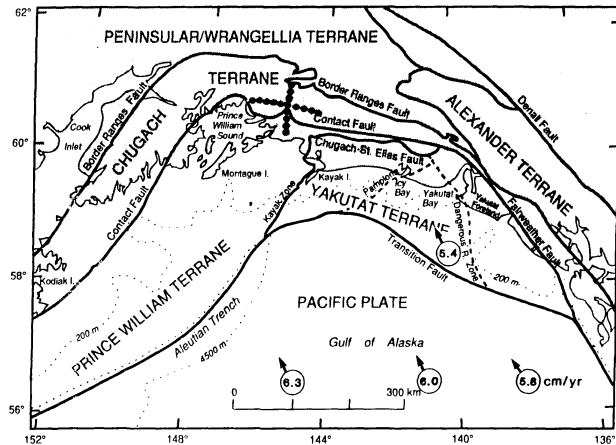
Figure 1. Regional tectonic map of southern Alaska [modified from Jones et al. [1981; 1987]. Arrows indicate relative motion between Pacific and North American plates [Minster et al., 1974; Lahr and Plafker, 1980].

2

seismic refraction profiles from the U.S. Geological Survey's Trans-Alaska Crustal Transect (TACT) using two-dimensional asymptotic ray theory (Figure 2). Chapter 1 provides a geologic and tectonic framework with which to view the seismic refraction data. Here the major tectonic problems are presented. The refraction data is then used to resolve or at least to provide constraints for some of these problems.

Chapters 2 and 3 contain manuscripts which were written as distinct entities for publication in professional journals and are included here with minor revisions. The first paper, *Upper Crustal Structure of the Accreted Chugach Terrane, Alaska,* deals exclusively with the Chugach refraction profile, a 135-km line which consists of four reversed shots and which follows the regional E-W strike of structures in the Chugach Mountains. The paper was co-authored by Dr. Alan Levander and published in the *Journal of Geophysical Research, vol. 94, B4, 4457-4466, 1989.* Dr. Levander's role was to guide the interpretation and data analysis by offering expertise in methodology and computing facilities at Rice University. He also contributed editorial suggestions. The second paper, Chapter 3, contains an analysis and interpretation of the Cordova Peak seismic refraction profile, a 126-km line which consists of five reversed shots and which is parallel to the N-S regional structural dip. The Cordova Peak manuscript is currently in preparation for submission to the *Journal of Geophysical Research.* Although the primary focus of

Figure 2. Generalized geologic map of southern Alaska showing locations of TACT seismic refraction profiles. Heavy solid lines correspond to cross sections in Figures 10 and 23. Chugach refraction profile extends from SP 17 to SP 20; Cordova Peak profile extends from SP 11 to SP 37. Small dots indicate receiver locations; large crosses indicate shot points 17, 18, 19, and 20 in strike profile and shotpoints 11, 12, 19, 38 and 38 in dip profile. Units Kvv, Kvg, Kjm = metavolcanic rocks; Kvs = metamorphosed flysch; Kvg = rocks in Chugach Metamorphic Complex; Tg = igneous intrusive rocks; To, Tl = sedimentary and volcanic rocks.

GENERALIZED GEOLOGIC MAP

Modified from: Winkler and others, 1981
Plafker, 1987
Plafker and others, 1989

Border Ranges Fault

Valdez

Prince William Sound

PRINCE WILLIAM TERRANE

GULF OF ALASKA

YAKUTAT TERRANE

SCALE
0   25 KM

LEGEND

WRANGELLIA-PENINSULA TERRANE

Glaciers

Unconsolidated deposits

QTw Wrangell lavas

— Fault
&
— · — Inferred Fault

Wrangellia terrane
Haley Crk. terrane

Peninsular terrane

CHUGACH TERRANE

Valdez Group

Kvs

Kvv

Kvm

Kvg

McHugh Complex

Kjm

Liberty Creek

Jlc

Iceberg Lake

Jlc

PRINCE WILLIAM TERRANE

Orca Group

To

Tg

YAKUTAT TERRANE

Tl

the second manuscript is the interpretation of data from the Cordova Peak seismic refraction line, the paper incorporates the model for the Chugach profile, derived for the previous paper, into a three-dimensional picture of the subsurface structure in the vicinity of the TACT corridor. In addition to the possible geologic interpretations presented in Cordova Peak paper, an attempt is made to integrate the two seismic models with other geophysical data, such as that from potential field and physical properties studies.

The interpretations and possible models of upper crustal structure presented in the two manuscripts are woven together in Chapter 4. In this chapter, the major conclusions drawn from analyses of the two seismic refraction profiles are outlined and discussed within the context of the regional geologic and tectonic setting. An ancilliary discussion concerning the methodology and accuracy of asymptotic ray theory used in the interpretation is given in the Appendix.

INTRODUCTION

Overview.

The Chugach and Prince William terranes of southern Alaska form part of a tectonically complex transition zone which is situated at the eastern end of the convergent North American-Pacific plate boundary (Figures 1 and 2). In the western portion of the zone, convergent structures dominate, while in the east, transform motion is distributed along a series of discrete fault zones. The subsurface relationships of the two terranes to each other and to the currently subducting plate have been the focus of much research but remain uncertain.

Determining the subsurface structure of southern Alaska is an important step towards developing an understanding of the complex tectonics and geologic history of this area and of accretionary processes in general. In an effort to gain such insight, the U.S. Geological Survey began the Trans-Alaska Crustal Transect (TACT), an integrated program of geological studies and crustal seismic investigations which started in the Gulf of Alaska and continued northward through the Chugach Mountains and beyond. The focus of the following study is the interpretation of two of the TACT seismic refraction lines, the Chugach and the Cordova Peak profiles, which were shot in southern Alaska in 1984 and 1985.

6

Experiment details.

The objective of the seismic refraction experiment was to provide constraints on the crustal structure of southern Alaska beneath the Chugach and Prince William terranes. The orientations of the profiles were chosen to match, as closely as possible, the regional strike and dip directions. Accessibility and roads in southern Alaska are limited, however, and place major restrictions on the profile locations.

The 135-km Chugach profile consists of four reversed shots spaced at intervals of 25-60 km. It is intersected by the 126-km Cordova Peak profile, which consists of five reversed shots spaced at intervals of 25-40 km. Shots in the Chugach profile were located exclusively within rocks of the Chugach terrane, whereas those in the Cordova Peak profile sampled both the Chugach and the Prince William terranes. All shots were recorded by 120 portable seismic recorders spaced at approximately 1-km intervals. Recorders were laid out in a fixed array for each profile to allow ray paths from shots to cross-sample subsurface structures and to enable a two-dimensional solution to be calculated for those areas with reversed coverage.

Since the Chugach profile follows the regional strike, it was assumed that the data would image relatively flat-lying, homogeneous layers and would therefore provide a "control" on the crustal velocity structure of the terrane for use in the interpretation of the dip profile. The Cordova Peak profile crosses, from north to south, the Chugach terrane, the Contact fault zone and the Prince William terrane.

has been described as a suture boundary which separates the Chugach terrane from the Prince William terrane [Winkler and Plafker, 1981: Plafker et al., 1986]. One objective of the Cordova Peak refraction experiment was to provide information on the nature of this boundary in the subsurface.

The profile lengths as well as the shot and receiver spacings were chosen to image as deeply as possible without sacrificing resolution within the upper crustal layers. A length of approximately 130 km can usually image, to some degree, the upper 20-25 km of crust. The shot and receiver spacing used in the experiments was sufficient to identify major lithologic interfaces but did not permit modelling of small features (< 5-10 km in length) with much detail. With this kind of resolution, one might hope to gain some insight into the following problems: 1) the subsurface structure of accreted rocks and their tectonic development, 2) the nature of terrane boundaries, and 3) the geometrical relationships between lower and upper crustal structure.

CHAPTER 1: GEOLOGIC AND TECTONIC SETTING

Although the TACT corridor covers only a small area of the overall tectonic regime of southern Alaska, it occupies a strategic position between a classic convergent margin, represented by subduction of the Pacific plate along the Aleutian trench, and a textbook transform margin, represented by right-lateral strike-slip motion along the Fairweather fault system. In addition, the TACT corridor is located near the Yakutat terrane, which provides a modern example of terrane accretion and continental collision. The transect affords a glimpse into the dynamic processes of a tectonically complex zone, the implications of which extend beyond the area of the TACT project.

1.1 Relative plate motions.

Figure 1 illustrates the relative motion vectors between the Pacific and North American plates in the Gulf of Alaska region. The motions are based on the RM1 model proposed by Minster et al. [1974] in which relative motion is described by a small circle rotation about an Euler pole. The average rate of relative motion between these two plates (6 cm/yr) cannot be attributed entirely to a single, sharply

9

defined boundary, as is indicated by recent motion on faults and internal
deformation of continental rocks inland of the Gulf of Alaska [Jacob, 1986].

Estimated relative motion rates shown for different areas in Figure 1 illustrate a
complex tectonic problem. The Yakutat terrane is thought to be moving with the
Pacific plate but at a slightly slower speed [Lahr and Plafker, 1980; Jacob, 1986].
These estimates are in agreement with recent very long baseline inferometry (VLBI)
data [Ma et al., 1989]. The difference between rates for the Yakutat terrane and for
the Pacific plate in the eastern portion of the Gulf of Alaska range from 0.4-1.0
cm/yr [Lahr and Plafker, 1980; Ma, et al., 1989]. This difference in relative motion
needs to be accounted for by internal deformation of the Yakutat terrane and/or by
movement on reactivated or newly-developed faults [Jacob, 1986]. In a more recent
study, Plafker [1987] suggests that previously proposed estimates of convergence
and displacement are too low. The rate of convergence is important for determining
how much of the Yakutat terrane has been subducted. To understand the plate
tectonics of southern Alaska, it is important to know the subsurface boundaries of
the Yakutat terrane and its structural relationship to the accreted Chugach and Prince
William terranes.

1.2 Terrane descriptions.

The Chugach and Prince William terranes are part of an accretionary complex which extends from a convergent tectonic regime in the west to a transform margin in the east (Figure 1). To the north, the Chugach terrane is bounded by the Border Ranges fault system, a zone of northward dipping faults along which the Chugach terrane has been thrust beneath the older composite Peninsular/Wrangellia terrane [Winkler et al., 1981]. To the south lies the Contact fault system, which is thought to form a steeply dipping suture boundary between the Chugach and Prince William terranes [Winkler and Plafker, 1981]; its attitude at depth and its vertical extent are not known. The Prince William terrane is bounded to the east by the younger Yakutat terrane and to the south by the Aleutian trench, where subduction of the Pacific plate begins.

1.2.1 Chugach terrane.

The Chugach terrane is composed of highly deformed, accreted and metamorphosed clastic sedimentary rock and oceanic crust (Figure 2). It has been divided, from north to south, into three major fault-bounded sequences: the Upper Jurassic or older Liberty Creek schists, the Upper Jurassic or older to Lower Cretaceous McHugh Complex and the Upper Cretaceous Valdez Group [Winkler et al., 1981; Silberling and Jones, 1984; Plafker et al., 1989].

The Liberty Creek schists are exposed locally along the northern margin of the Chugach terrane. They comprise an oceanic assemblage of basalt flows, breccia and tuff, with minor amounts of marine sedimentary rocks, which were regionally metamorphosed to greenschist and locally blueschist facies at estimated depths of 22-36 km [Winkler et al., 1981; Turner, 1981]. Thickness of the Liberty Creek schist sequence is estimated to be at least 5 km [Plafker et al., 1989]. Its contact with the Peninsular terrane on the north is marked by a shear zone of highly deformed ultramafic rocks [Plafker et al., 1989]. To the south, the contact of the Liberty Creek schists with the McHugh Complex is identified by a zone of highly sheared and altered mafic and ultramafic rocks [Plafker et al., 1989].

The McHugh Complex in the area of the transect corridor consists mainly of faulted and metamorphosed tholeiitic pillow basalts and other mafic volcanic rocks, with minor amounts of associated pelagic and continent-derived siliciclastic sediments [Winkler et al., 1981]. Rocks throughout most of the unit have been metamorphosed to prehnite-pumpellyite facies as the result of subduction to depths less than 13 km and of temperature increases not in excess of 300 degrees C [Plafker et al.,1989; Turner, 1981]. Rocks in the McHugh Complex show some evidence of south-verging structure, but lack the degree of schistosity seen to the south and north [Plafker et al., 1989]. Because of its structural complexity, stratigraphic thickness of the McHugh Complex is not known; its estimated structural thickness is about 20

km [Plafker et al., 1989]. The McHugh Complex is juxtaposed with rocks of the Valdez Group along its faulted southern margin.

The Valdez Group consists of a thick wedge of accreted sedimentary and volcanic rocks which were later exposed to low-pressure/high-temperature metamorphism [Hudson and Plafker, 1982; Sisson and Hollister, 1988]. Metasedimentary rocks of the Valdez Group are primarily turbidites consisting of interbedded graywacke and pelite [Winkler et al., 1981]. Metavolcanic rocks are mainly tholeiitic flow and pillow basalts, which increase in abundance southward towards the Contact fault zone [Winkler et al., 1981; Winkler and Plafker, 1981]. Clastic sedimentary rocks, predominantly sandstones, are thought to have been deposited in a deep-sea fan directly onto oceanic crust, represented by basalts and related volcanic rocks [Plafker et al., 1989]. The Valdez Group was thrust beneath the McHugh Complex and is highly deformed along this boundary [Plafker et al., 1989]. In some areas, it underlies the Haley Creek terrane, a thin, rootless sheet composed of plutonic and metamorphic rocks [Wallace, 1985]. Progressive metamorphism of the Valdez Group began in Early to Middle Eocene time [Plafker et al.,1989]. Near the west end of the Chugach refraction profile, rocks of the Chugach terrane have been metamorphosed to greenschist facies [Hudson and Plafker, 1982]. The metamorphic grade of the Valdez Group increases eastward to amphibolite facies in the Chugach Metamorphic Complex, located east of the

Copper River [Hudson and Plafker, 1982]. The stratigraphic thickness of the Valdez

Group is estimated at several kilometers; its structural thickness is estimated to be at

most 20 km [Plafker et al., 1989]. Along its southern edge, the Valdez Group is

bounded by the Contact fault system, which separates the Chugach terrane from the

younger Prince William terrane.

1.2.2 Prince William terrane.

The Prince William terrane contains rocks of the Orca Group, a late Paleocene

to Eocene deep-sea fan deposit interbedded with pillow and flow basalts, tuff-

breccia and minor pelagic sediments, and intruded by diabase sills [Winkler and

Plafker, 1981; Plafker, 1987]. The Orca Group, which forms the basement of the

Prince William terrane, was accreted to the Chugach terrane and metamorphosed to

zeolite to greenschist facies about 50 Ma ago [Plafker, 1987]. Since that time, no

major horizontal displacement has occurred along the suture zone [Plafker, 1987].

The stratigraphic thickness of the Orca Group is estimated to be 6-10 km [Winkler

and Plafker, 1981].

Overlying the Orca Group are Late Eocene or older to Quaternary siliciclastic

sedimentary rocks which were deposited in shelf and slope basins on a subsiding

continental margin and which comprise as much as 4 km of section [Plafker, 1987].

Unlike rocks of the Orca Group, these more recent sedimentary rocks are relatively

undeformed and were most likely deposited near or at their present latitude [Rau et al., 1983; Plafker, 1987].

Similarity in the lithology and depositional history between rocks of the Chugach and the Prince William terranes has raised some question as to the distinction between the two terranes and the position of their boundary [Dumoulin, 1988]. In the area near western Prince William Sound, little metamorphism or deformation is observed within the terranes and no well-defined boundary between them exists [Dumoulin, 1988]. It has been argued, therefore, that the minor differences seen in the rocks of the two terranes in other areas may simply reflect a metamorphic gradient and that the Contact fault zone may be no more than a series of thrust faults in a developing accretionary prism.

1.2.3 <u>Yakutat terrane</u>.

The Yakutat terrane lies to the east of and structurally below the Prince William terrane on the Gulf of Alaska margin. It is bounded to the east by the Fairweather fault system, to the north by the Chugach-St. Elias fault system, to the west by the Kayak Island zone and to the south by the Transition Fault (Figure 1). The precise location and character of the subsurface boundary between the Prince William and Yakutat terranes, however, is unknown. Basement rocks of the Yakutat terrane west of the Dangerous River zone, an old boundary which separates different types of

terrane basement, consist of Paleogene oceanic crust [Plafker, 1987]. East of the Dangerous River zone, basement rocks are continentally derived and consist of the upper Mesozoic flysch and melange of the Yakutat Group [Plafker, 1987]. The flysch sequence was intruded by Eocene felsic rocks and may be correlative with the flysch sequence of the Valdez Group [Plafker et. al., 1989].

Overlying the basement rocks are primarily Lower Eocene to Quaternary clastic sequences [Winkler and Plafker, 1981; Plafker, 1987]. Paleogene sandstones indicate an igneous and high-grade metamorphic provenance, whereas the upper Cenozoic sequence is thought to be derived locally from erosion of the Chugach and St. Elias Mountains, as the result of uplift from collision and underthrusting of the Yakutat terrane [Plafker, 1987]. This history would suggest that the Yakutat terrane was attached to the Prince William terrane by middle to late Cenozoic time.

The Pamplona zone (Figure 1) is a major tectonic boundary which separates an active fold-and-thrust belt in the northwestern part of the Yakutat terrane from the relatively undeformed southeastern part of the terrane [Plafker, 1987]. This boundary is clearly expressed in the offshore seismic reflection data collected to the southeast of the TACT corridor [Bruns, 1983].

1.3 Eocene plutonism.

Felsic to intermediate hypabyssal and plutonic rocks were intruded into the Chugach and Prince William terranes in Eocene time, following the start of regional metamorphism of the Valdez Group [Winkler et al., 1981; Plafker et al., 1989]. They consist of dikes, sills and small stocks, ranging from tens of meters (for dikes) to a few square kilometers (for small stocks) [Plafker et al., 1989]. Intrusion of these rocks provided a thermal pulse which contributed to progressive low pressure/high temperature metamorphism in areas surrounding the intrusions [Sisson and Hollister, 1988].

Intrusions near the transect consist mainly of steeply dipping dikes, dike swarms and small stocks [Plafker et al., 1989]. The number and size of intrusions increase south and east of the transect profiles through the Chugach and Prince William terranes. The hypabyssal rocks are younger than the Paleocene to Eocene Orca Group [Plafker et al., 1989]. They also post-date major motion along the Border Ranges and Contact fault zones, and are seen to crosscut the latter east of the transect [Winkler and Plafker, 1981].

1.4 Summary of geologic and tectonic history.

Geologic studies indicate that the Chugach terrane consists of clastic

sedimentary rocks which were deposited along a continental margin onto oceanic rocks at a location to the south of their current latitude. They were later transported northward to their present location. accreted and deformed in several stages which are estimated to have begun in Cretaceous and continued to Tertiary time [Plafker, 1987].

Prince William terrane rocks were deposited in a deep-sea fan complex onto oceanic volcanic rocks. Paleomagnetic studies indicate that the Orca Group rocks, which form the basement of the Prince William terrane, could have travelled from as far as 40 degrees south of their present location [Plumley and Plafker, 1983]. Estimates for accretion of the Prince William terrane to North America range from Early to Middle Eocene time [von Huene et al., 1985; Plafker et al., 1989]. Paleogene strata overlying the Orca Group were thought to be deposited in place [Plafker et al., 1989].

Rocks of the Chugach and Prince William terranes were intruded by felsic to intermediate hypabyssal and plutonic rocks in an Early to Middle Eocene event. Intrusions form dikes, sills and small stocks which increase in both number and size south and east of the transect corridor. Intrusions are responsible for some contact metamorphism, particularly in the Chugach Metamorphic Complex [Hudson and Plafker, 1982; Sisson and Hollister. 1988].

Rocks of the Yakutat terrane form two distinct segments: in the western portion, basement rocks are oceanic and to the east, continental margin flysch. Geologic studies suggest that the Yakutat terrane was transported approximately 400-600 km northward to its present position by right-lateral strike-slip motion along the Fairweather and Queen Charlotte fault systems [von Huene, 1985; Plafker, 1987]. It reached its current location and was thrust beneath the Prince William terrane by Early Eocene time [Plafker, 1987]. The Yakutat terrane is currently accreting to southern Alaska.

The previous discussion of the Chugach, Prince William and Yakutat terranes of southern Alaska brings to light several questions which are important to an interpretation of the seismic refraction data: 1) Are the Chugach and Prince William terranes distinct geologic entities with different histories? 2) What is the nature of the boundary between the two terranes and how is it expressed in the seismic record? 3) What structural features seen in surface geology are seen in the refraction data? 4) Where are the boundaries of the subducting Yakutat terrane? 5) How do deep structural relationships affect observations in the upper crust and vice versa? and 6) How well can the seismic refraction data help to clarify or constrain the interpretations made from geological data and other geophysical data sets?

CHAPTER 2: CHUGACH SEISMIC REFRACTION PROFILE[1]

2.1 Abstract.

We have developed a model for the upper crustal structure of the Chugach terrane of southcentral Alaska from U.S. Geological Survey seismic refraction data using two-dimensional asymptotic ray tracing. The refraction profile, acquired as part of the Trans-Alaska Crustal Transect program, extends approximately 135 km in an east-west direction along the local strike of the Chugach Mountains. The refraction survey consists of four shots, recorded by 120 portable seismic instruments spaced at 1-km intervals. We observe a velocity-depth profile which has unusually high velocities at shallow depths and at least two velocity reversals. The average velocity increases from 4.0 km/s at the surface to 6.9 km/s at a depth of 9 km. Near-surface velocities in Cretaceous Valdez Group rocks increase eastward following the metamorphic gradient observed by Hudson and Plafker [1982]. Lower layers may be correlated with rocks mapped to the south of the Contact fault zone, a suture boundary between the Chugach and Prince William terranes, and with units not having surface expression. The first

---

[1]Chapter 2 contains the text of the manuscript, *Upper Crustal Structure of the Accreted Chugach Terrane, Alaska* by Wolf and Levander as published in the *Journal of Geophysical Research, 94, 4457-4466, 1989.* To avoid repetition, the reader may wish to proceed to the Data and Analysis section (2.4).

velocity reversal occurs at a depth of 9 km. This 1- to 2-km zone has velocities which vary laterally from 6.0 to 6.9 km/s and pinches out to the east in the profile. This unit may represent a zone comprising Tertiary intrusions and country rock. It is underlain at a depth of 10 km by a layer with velocities of 7.20-7.23 km/s. The second velocity reversal occurs at a depth of 12 km. Velocities within this layer range from 6.6 to 6.7 km/s and may correlate with underplated oceanic crust. Higher velocities of 7.35-7.40 km/s are attributed to a thin unit at a 14-km depth associated with ultramafic and mafic rocks. The deepest unit is modelled as a 5-km layer having velocities of 7.20-7.25 km/s. This layer may be underplated Prince William terrane rocks, oceanic crust, or some portion of the Yakutat terrane. The refraction data alone do not resolve deeper structure.

2.2 Introduction.

The Chugach Mountains of southern Alaska are located north of the Gulf of Alaska and east of Anchorage along the convergent North American-Pacific plate boundary. Crustal structure of this area involves compressional tectonics due to subduction of the Pacific plate beneath the North American plate. Geologic mapping indicates the region comprises three distinct terranes: the Prince William terrane, the Chugach terrane and the Peninsular/Wrangellia terrane (Silberling and Jones, 1984). To understand better the geologic history and subsurface structure of these terranes and

of Alaska as a whole, the U.S. Geological Survey began a program of geologic mapping and crustal seismic investigations (Trans-Alaska Crustal Transect (TACT)) which started in the Gulf of Alaska and continued northward through the Chugach Mountains and beyond. A 135-km seismic refraction profile through the Chugach terrane, shot in 1985, parallels the regional strike of the Chugach Mountains (Figure 1). By integrating geologic surface mapping [Winkler et al., 1981; Plafker et al., 1986; Nokleberg et al., 1989] with our seismic refraction interpretation, we have correlated the subsurface velocity model with different geologic units for the Chugach area. We observe unusually high velocities (4.0 to 6.9 km/s) within the upper 9 km of crust. Layers extending to a depth of 5 km are correlated with Cretaceous Valdez Group rocks which crop out along the refraction line and to the south. These layers are followed by a 3- to 4-km unit having an average velocity of 6.9 km/s, with localized areas having a velocity of 7.4 km/s. We observe two velocity reversals below the third layer. Velocities in the first reversal are laterally variable and range from 6.05 to 6.90 km/s. Velocities within the second are laterally consistent, averaging 6.65 km/s within the 2-km-thick layer.

2.3 Geologic Setting.

The Chugach terrane is a Mesozoic accretionary complex in a modern compressional tectonic regime. It is bounded to the north by the Border Ranges fault

system, a zone of northward dipping faults which show the Chugach terrane

underthrust beneath the older composite Pennisular/Wrangellia terrane [Winkler et al.,

1981; Wallace, 1981; 1984]. To the south, the Chugach terrane is bounded by the

Contact fault system, a zone of northward dipping faults which appear to separate the

Chugach terrane from the younger Prince William terrane [Winkler and Plafker, 1981].

The structural trend in the area is approximately east-west.

The Chugach terrane has been divided into three major sequences: the Upper

Jurassic or older Liberty Creek schists, the Upper Jurassic to Lower Cretaceous

McHugh Complex, and the Upper Cretaceous Valdez Group [Winkler et al., 1981;

Silberling and Jones, 1984]. The Chugach seismic refraction profile lies within the

Valdez Group (Figure 1), an accretionary prism consisting of interbedded graywackes,

siltstones and mudstones, with minor mafic volcanics and conglomerates [Winkler et

al., 1981]. Rocks of the Valdez Group are accreted sediments which were exposed to

low-pressure/high-temperature metamorphism subsequent to deposition [Hudson and

Plafker, 1982; Sisson and Hollister, 1988; Sisson et al., 1989]. Near the west end of

the refraction profile, at shotpoint 17, Valdez Group rocks have been metamorphosed

to greenschist facies. The metamorphic grade increases eastward to amphibolite facies

in the area beyond the Copper River. This area, known as the Chugach Metamorphic

Complex, has an elongate surface expression approximately 25 km wide and at least

180 km wide [Hudson and Plafker, 1982]. Rocks in the complex are intruded by felsic to intermediate sills, dikes and plutons.

2.4 Data and analysis.

The Chugach profile lies approximately west-east, 135 km from shot point 17 to shot point 20, with a slight southward bend in the area of shot point 18 (Figure 2). It is a reversed profile consisting of four shots, each recorded by approximately 120 portable seismic recorders spaced at 1-km intervals and laid out in a fixed array [Daley et al., 1985]. Approximately 30 km west of shot point 20, the seismic line crosses the Copper River, which marks the western boundary of the Chugach Metamorphic Complex [Hudson and Plafker, 1982]. All shot points lie within Valdez Group rocks, but only shot point 20 is located within the complex. The profile is aligned with the regional east-west structural trend. The four shots of the Chugach profile have been interpreted using two-dimensional ray tracing based on asymptotic ray theory [Cerveny et al., 1977; Luetgert, 1987] to match both travel times and amplitudes. Travel times were fit to within 0.05 s, except in places where the limitations of the ray tracing algorithm would not allow small-scale modeling of the velocity structure.

Synthetic seismograms were used to match amplitudes and refine the velocity model. Ray synthetic seismograms were produced by two different programs: SEIS83 [Cerveny and Psencik, 1984] and R86PLT [Luetgert, 1987]. Field records and

synthetic seismograms are shown as trace-normalized record sections, with a reduction velocity of 6 km/s (Figures 3, 4, 5, and 6). Only results using R86PLT are shown in Figures 3-6.

Figures 3, 4, 5, 6 contain field data from each shot point with calculated travel times and synthetic seismograms from the best-fit model. The best-fit to travel times and amplitudes is the result of over 50 iterations of adjustments to the model. Each figure contains reduced travel time curves overlain on the record section, a velocity-depth profile for the appropriate shot point, a synthetic record section, and a ray diagram. Ray diagrams are included to illustrate the areas sampled in different layers, but for simplification, only representative rays are shown. The ray trace models are plotted with a 2x vertical exaggeration; sea level corresponds to a 2-km depth in the model. Topography, as determined from receiver elevations, is included in the model.

The first layer is 1-2 km thick and locally contains large pockets of unconsolidated sediment. Surface compressional velocities range from a low of 2.1 km/s, associated with sedimentary rocks, to a high of 5.6 km/s near exposed bedrock. Delays in travel times and some complexity in the record section near shot point 18 indicate the presence of a 1-km-thick sedimentary pile to the west of the shot point (Figures 3 and 4). Primary arrivals from the first layer immediately to the west of shot point 18 show substantially lower velocities than those immediately to the east. The presence of large bodies of ice scattered along the profile may contribute to lateral
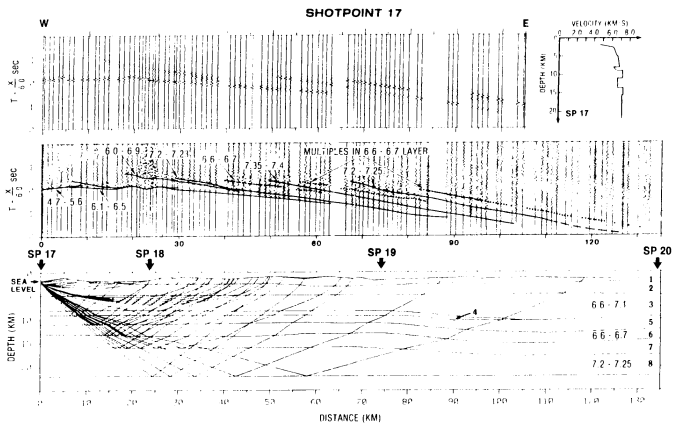
Figure 3. Reduced-time record section with calculated travel time curves, synthetic record section, ray diagram, and velocity-depth profile for SP17. Calculated travel times from same branch are connected and overlie trace-normalized record section. Velocities given in kilometers per second. Arrivals from the second low-velocity zone as well as pegleg multiples are indicated by dotted lines. Some curves are omitted to avoid clutter in the diagram. Amplitudes are not modeled beyond 100 km because of limited accuracy at long offsets (see text).
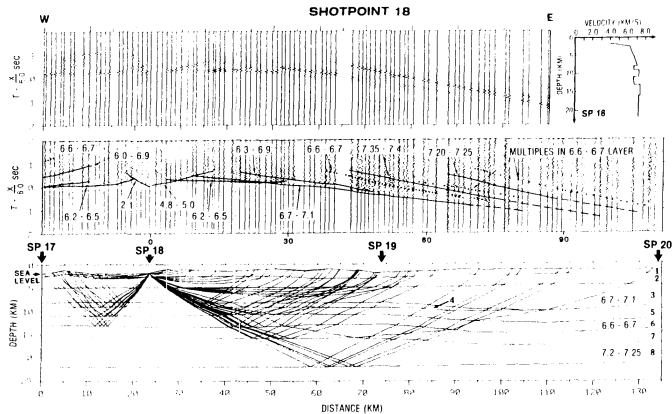
Figure 4. Reduced-time record section with calculated travel time curves, synthetic record section, ray diagram, and velocity-depth profile for SP18. Calculated travel times from same branch are connected and overlie trace-normalized record section. Velocities given in kilometers per second. Arrivals from the second low-velocity zone as well as pegleg multiples are indicated by dotted lines. Some curves are omitted to avoid clutter in the diagram. Amplitudes are not modeled beyond 100 km because of limited accuracy at long offsets (see text).

27
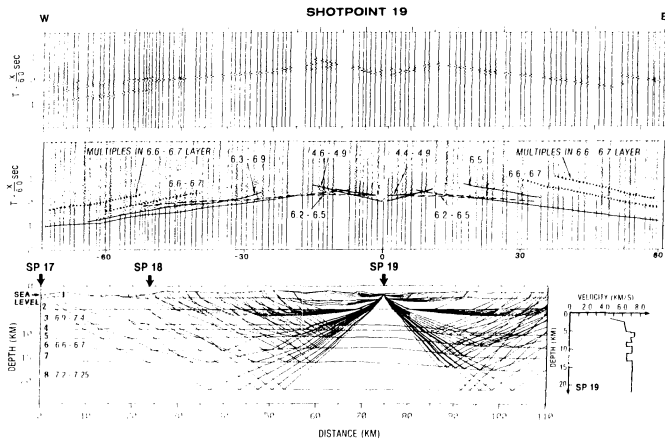
Figure 5. Reduced-time record section with calculated travel time curves, synthetic record section, ray diagram, and velocity-depth profile for SP19. Calculated travel times from same branch are connected and overlie trace-normalized record section. Velocities given in kilometers per second. Arrivals from the second low-velocity zone as well as pegleg multiples are indicated by dotted lines. Some curves are omitted to avoid clutter in the diagram. Amplitudes are not modeled beyond 100 km because of limited accuracy at long offsets (see text).

28
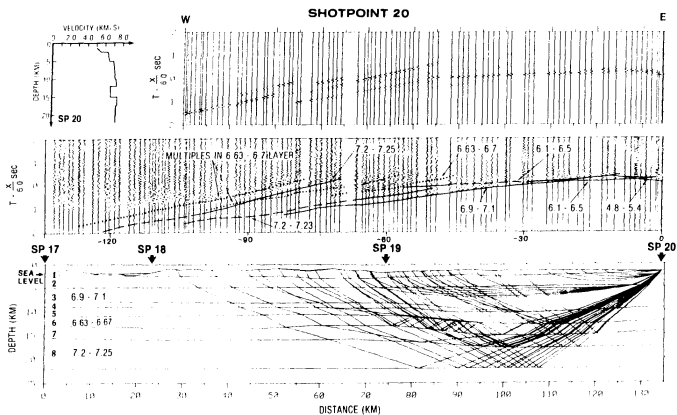
Figure 6. Reduced-time record section with calculated travel time curves, synthetic record section, ray diagram, and velocity-depth profile for SP20. Calculated travel times from same branch are connected and overlie trace-normalized record section. Velocities given in kilometers per second. Arrivals from the second low-velocity zone as well as pegleg multiples are indicated by dotted lines. Some curves are omitted to avoid clutter in the diagram. Amplitudes are not modeled beyond 100 km because of limited accuracy at long offsets (see text).

velocity variations in the near surface. The second layer in the model is 1-2 km thick and has velocities which range from 6.1 to 6.5 km/s. There is some lateral variation in the velocity of this layer, particularly in the area near shot point 19. Velocities in shallow layers increase eastward throughout the model, with the first layer showing more variability than the second.

The third layer is modelled as 4-5 km in thickness, with velocities ranging from 6.6 to 7.1 km/s. This layer thins slightly to the west in the region between shot points 19 and 17. First arrivals from this unit indicate the presence of discontinuous high-velocity material throughout the third layer. Travel times at offsets of approximately 40 km to the east and west of shot point 19 can be better modelled by including laterally limited high-velocity features, about 1-2 km in thickness and several kilometers in length, within the layer. These high-velocity features were modelled using the Cerveny and Psencik program, SEIS83. They are estimated to have velocities of 7.4 km/s and account for the discrepancy between calculated and observed travel times of primary arrivals at offsets of 15-40 km (Figure 5).

Arrivals from layer 4 on the shot point records suggest a change in the geometry of the units. Layers form a broad arch beneath shot point 19, dipping slightly more to the east than to the west. The fourth layer is modelled as a thin unit in which the velocity ranges from 6.0 to 6.8 km/s. The presence of this low-velocity layer is indicated in the record sections from shot points (SP) 17, 18, and 19 by high-amplitude

second arrivals at offsets of approximately 18-40 km and reduced times of 0.0-0.5 s. In the record from SP17, high-amplitude second arrivals occur at offsets of 18-37 km (Figure 3). In the record from SP18, high-amplitude second arrivals appear at similar distances on both sides of the shot point (Figure 4). In the record from SP19, however, no symmetry in the offsets of high-amplitude second arrivals is observed (Figure 5). To the east, the first of these arrivals is seen at an offset of approximately 18 km and 0.5 s (labeled as 6.5 km/s phase), but to the west, high-amplitude second arrivals are not observed until approximately 28 km and 0.25 s (labeled as 6.3-6.9 phase). Arrivals attributed to the first low-velocity zone are not evident in the record section from shot point 20 (Figure 6). The first later-arriving high-amplitude pulse does not occur until an offset of 50 km and 0.0 s.

Because continuous high-amplitude second arrivals from the low-velocity layer are not seen in the data from all shots, the layer is assumed to be laterally limited (Figure 7). Layer 4 is therefore shown to pinch out approximately 30 km east of shot point 19. Laterally varying velocities in layer 4 produce high-amplitudes in some areas and low amplitudes in others. Arrivals from the low-velocity layer are often coincident with arrivals from a high-velocity layer beneath it, thus accounting for the amplitudes observed at some offsets. Models lacking the first low-velocity zone fail to produce the high-amplitude second arrivals seen in the data from shot points 17, 18, and 19. The preferred model, which includes this laterally limited fourth layer, produces better
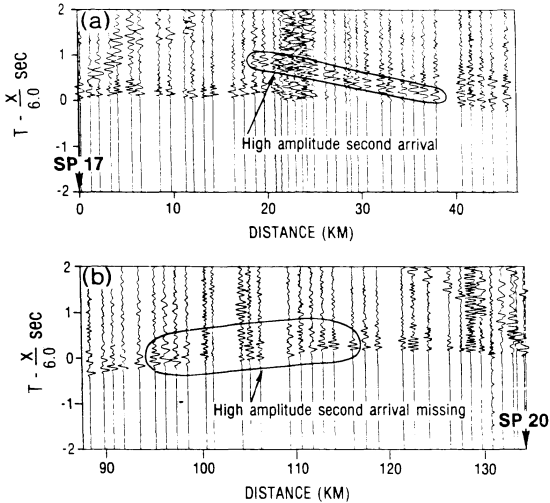
Figure 7. Comparison of observed data from shot points 17 and 20. High-amplitude second arrivals appearing 20-37 km from SP 17 at 0.5 s reduced time are attributed to the low-velocity layer (Figure 7a). A similar phase is absent in the record from SP 20 at comparable ranges and travel times, suggesting that the layer does not extend eastward to SP 20 (Figure 7b).

amplitude matches in some areas. The inability of ray methods to model accurately some types of complex structures made it difficult to match amplitudes to the east of shot point 19, where the fourth layer pinches out. An example of this limitation is discussed later.

Layer 5 is a high-velocity layer which underlies the low-velocity zone. It is approximately 2 km thick, with velocities ranging from 7.20 to 7.23 km/s. The high velocities in layer 5 are required to produce first arrivals beyond 60 km, the offset at which first arrivals from layer 3 die out (Figures 3, 4, 5, and 6). The lack of prominent first arrivals beyond 80 km in the record sections suggests that the fifth layer is thin. Large-amplitude second arrivals at offsets of approximately 60 km and 0.0 s (labeled as 6.6-6.7 km/s phase) and delayed first arrivals in the observed data (Figures 3, 4, 5 and 6) indicate a second low-velocity zone beneath layer 5. The delay in travel times suggests that this second low-velocity zone, layer 6, is thicker than the first. The velocity of layer 6 ranges from 6.6-6.7 km/s, with little lateral variation.

Layer 7 has velocities which range from 7.35 to 7.40 km/s. Because the maximum velocity in this unit is not much higher than that in layer 5, refraction is weak, resulting in indistinct phases at offsets greater than 80 km. First arrivals appear in refractions where layer 7 velocities exceed those in layer 5 above. The data do not provide good constraints on the velocities or geometries beneath layer 6, as can be evidenced by the ray trace diagrams in Figures 3, 4, 5, and 6. Rays from reversed shots

which penetrate deeper layers do not illuminate much of the structure because they intersect in only a small area in the central part of the model.

Figure 8 illustrates the limitations of the modelling technique in matching the amplitudes of synthetic seismograms with field data. The effect of minor changes in model parameterization on trace-normalized synthetic seismograms is pronounced. Figure 8 shows the result of lowering the fourth interface (bottom of the third layer) by 0.10 km at a distance of 117 km in the model, just east of the pinchout of layer 4. Synthetic seismograms of the two models are very similar close to shot point 20, but the ray synthetic traces at long offsets are dramatically different. The reliability of ray synthetic seismograms at large offsets is questionable when the structures are thin and pinch out.

Original interpretations of the Chugach profile postulated the existence of four pairs of alternating low-/high-velocity layers [Page et al., 1986]. Shingled events in the record section provided the evidence for low-velocity layers [Fuis and Ambos, 1986; Wolf et al., 1986]. Further analysis has suggested that later "steps" in the travel time curves are multiple reflections within shallow low-velocity layers [E. Flueh et al., Crustal structure of the Chugach Mountains, southern Alaska: A study of pegleg multiples from a low-velocity zone, submitted to Journal of Geophysical Research, 1988]. Using ray trace methods, we have successfully matched travel times of some
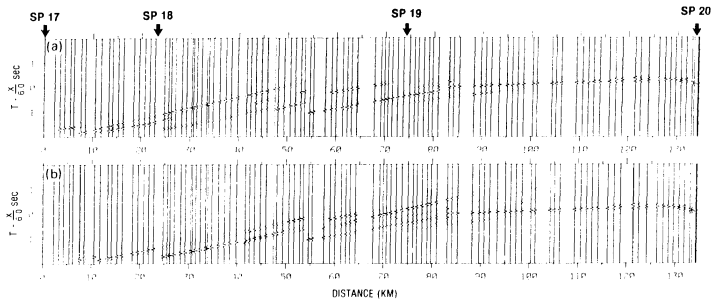
Figure 8. Comparison of two ray synthetic seismograms from SP20 showing effects of minor changes in the model: (a) the effect on synthetics of moving the lower boundary of layer 3 at 117 km in the model upwards by 0.1 km; (b) generated using the final model. Synthetics compare well at small offsets but are dramatically different at long offsets. The pinchout in layer 4 contributes to instability.

some later high-amplitude arrivals by modelling pegleg multiples within layer 6.
Readers are referred to work by E. Flueh et al. for detailed modelling of multiples
using reflectivity methods.

2.5 Geologic interpretations.

A geologic interpretation and detailed velocity model of the upper crustal
structure of the Chugach terrane are shown in Figures 9 and 10. Rocks at the surface
along the length of the profile have been mapped as Upper Cretaceous Valdez Group
rocks [Winkler and Plafker, 1981]. Near-surface features such as ice and pockets of
unconsolidated sediment contribute to substantial variation in shallow velocities
(Figure 9). In particular, the area immediately west of shot point 18 shows delays in
first arrivals, suggesting the existence of a 1-km-thick pocket of sediment. The
mapped western boundary of the Chugach Metamorphic Complex correlates well with
the increase in the shallow velocity structure to the east of shot point 19. Rocks within
this complex have been metamorphosed to amphibolite facies [Hudson and Plafker,
1982] and have average near-surface velocities of 5.0-5.3 km/s. Rocks outside the
complex (west of the Copper River) have been metamorphosed to greenschist facies
and have slightly lower average velocities (4.4-5.0 km/s) (Figure 9). Increasing
velocities to the east of shot point 19 occur only in the upper layers, evidence which
suggests the metamorphic gradient does not extend below a 5-km depth.
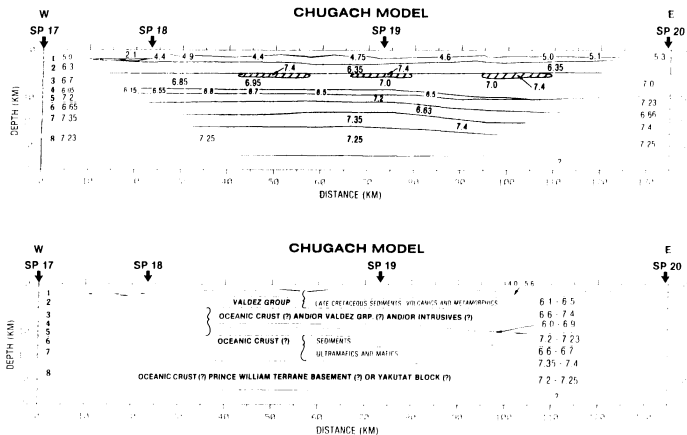
Figure 9. Detailed velocity model and possible geologic model based on seismic refraction interpretation from the USGS Chugach profile. Upper two layers are correlated with Valdez Group rocks. Layer 4 represents a low-velocity zone possibly containing Tertiary intrusives and country rock or oceanic sediments. Layer 5 is a high-velocity unit correlated with mafic or highly metamorphosed rocks. Layer 6 marks the second velocity reversal, which may correspond to underthrust oceanic sediments above ultramafic and mafic rocks. Although units below the third are shown to contain some Tertiary intrusives and Prince William terrane rocks, they could represent rocks not having surface expression. (See text for other interpretations.)

Figure 10. Fence diagram of geologic cross sections along lines indicated in Figure 2. East-west cross section corresponds to one geologic interpretation of refraction data from the Chugach terrane. Other interpretations are discussed in the text. Connecting cross sections are based on surface geology [Winkler and Plafker, 1981]. Earthquake foci indicate approximate location of subducting plate (western line from Stephens, et al., [1984]; eastern line from Wolf et al., [1986]). The Contact fault zone (CFZ) marks the boundary of the Chugach with the Prince William terrane to the south. The terrane boundary is inferred to extend to at least 10-12 km depth. Geometry of the CFZ is not well constrained but is modelled with a moderate northward dip, consistent with geologic and gravity data [Winkler and Plafker, 1981; Page et al., 1986]. Elongate features in layer 3 correspond to high-velocity areas discussed in text. Variation in shading east of SP 19 marks the boundary of the Chugach Metamorphic Complex [Hudson and Plafker, 1982].

CHUGACH TERRANE

INCREASING METAMORPHISM

PRINCE WILLIAM TERRANE
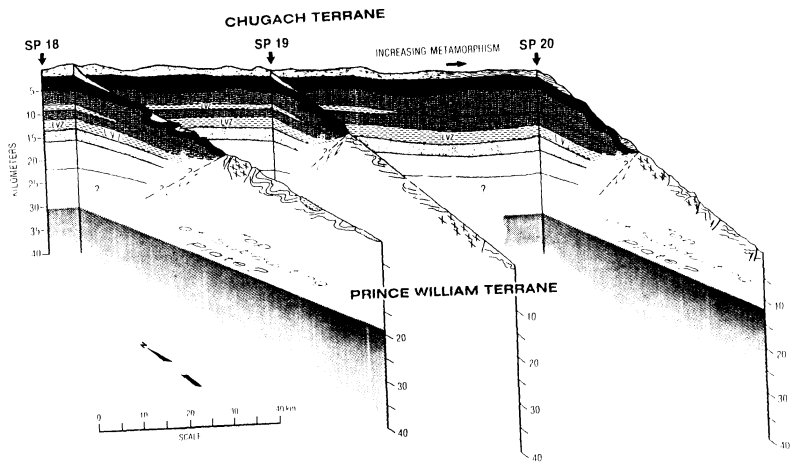
Approximately 10-25 km south of the Chugach profile is an elongate outcrop belt of Upper Cretaceous metavolcanic rocks, such as mafic metatuffs and massive greenstones, and metasedimentary rocks, such as marine argillites, sandstones, siltstones, and minor conglomerates [Winkler and Plafker, 1981]. Projecting this section downdip to the refraction line would place these rocks approximately within the upper 6 km of the model (Figure 10).

Based on the regional dip of units inferred from surface geology, the first two layers (approximately the upper 5-6 km of section) are correlated with Valdez Group rocks. Numerous thin mafic dikes and sills (up to 20 km long but tens of meters thick) have been mapped in these rocks [Winkler et al., 1981]. These small features increase the average velocity of a given layer and contribute to the lateral velocity variation within the first two units.

It is difficult to correlate the mapped surface geology with layers beneath the second. One possible interpretation is that layer 3, which has an average velocity of 6.9 km/s, contains subducted volcanic oceanic crust. The velocity of layer 3, as well as those of layers 5 and 7, is similar to that associated with gabbros in ophiolites and subducted mafic to ultramafic oceanic crust [Salisbury and Christensen, 1978; Spudich and Orcutt, 1980]. A second interpretation for layer 3 is that it contains Valdez Group rocks which are not exposed at the surface. The average velocity is compatible with ranges for highly metamorphosed rocks [Birch, 1960]. Localized regions of very high

velocity (7.4 km/s) from within layer 3 beneath shot point 19 are difficult to explain. These localized areas of high velocity may represent thin slivers of mantle material which were thrust into place by a downgoing plate or highly metamorphosed mafic to ultramafic rocks which were intruded during a syn-tectonic or post-tectonic event.

More than one interpretation can also be offered for layer 4, the first low-velocity layer. One possibility is that layer 4 consists of underplated oceanic sediment. The high-velocity material in layer 5 would then correspond to mafic oceanic crust. Ranges of velocities for oceanic crust and ophiolites at the depths of burial postulated for these units are in agreement with those made by Christensen [1978]. This velocity model and structural interpretation explain the time delays and high amplitudes in the record section. The model seems to presume, however, two relict subduction complexes above the currently subducting plate. Such a package of alternating low-/high-velocity pairs is not commonly seen in similar environments.

An alternative interpretation of layer 4 is that it contains Tertiary intrusive rocks equivalent to those appearing elsewhere at the surface. Both the Tertiary sedimentary rocks of the Prince William terrane and the Mesozoic metasedimentary rocks of the Chugach terrane have been intruded locally by Eocene felsic to intermediate rocks. Velocities in the first low-velocity layer vary laterally and may represent a composite of intrusions and surrounding flysch (Figure 9). Velocities in layer 5 are compatible

with those of layer 3 and suggest that layer 5 may be a downward continuation of that unit.

Possible geologic interpretations of the velocity model are shown in Figures 9 and 10. Layers 1 and 2 contain Valdez Group rocks exposed at the surface between the refraction line location and the Contact fault zone. Layers beneath the second do not project to the surface and therefore several geologic interpretations are indicated in Figure 9. Layer 3 could be a continuation of Valdez Group rocks or subducted oceanic volcanic rocks. Layer 4 is presented as a zone containing Tertiary intrusions and flysch or subducted oceanic sediments, underlain by a high-velocity layer (layer 5). Layer 6, the second low-velocity zone, is correlated with oceanic sediments but could possibly be underthrust Prince William terrane rocks from farther south. Higher velocities in layer 7 are compatible with mafic to ultramafic rocks which form the basement to sedimentary rocks in the Prince William terrane [Winkler and Plafker, 1981] or with relict subducted volcanic oceanic crust. Velocities below a 20-km depth in the model are not well constrained. These velocities could correspond to Prince William terrane basement rocks, to subducted oceanic crust or to rocks within the Yakutat terrane. The subsurface boundaries of the Yakutat terrane are not well known, and the relationship of the Yakutat terrane and the North American-Pacific plate boundary in southcentral Alaska is unclear [Bruns, 1983; Stephens et al., 1984].

2.6 Discussion and summary.

The velocity model we present for the Chugach refraction profile is grossly similar to that of Page et al. [1986]: a crustal velocity profile having unusually high velocities within the upper 10 km and two velocity reversals. We have refined the structure and velocity model for the upper crustal layers to a 22-km depth and offer several different geologic interpretations. Unfortunately, the data do not resolve the deeper structure. To match observed travel times and amplitudes, primary arrivals from lower layers must be delayed. Delays in travel times at long offsets from each of the shotpoints cannot be adequately accomodated by including many alternating low-high velocity pairs in the model, because arrivals from deeper high velocity layers appear at offsets greater than are observed in the data.

An attempt to tie the model presented here with the interpretation of the dip line to the north and south [Fuis and Ambos, 1986] and the mapped surface geology [Winkler and Plafker, 1981] is illustrated by the fence diagram in Figure 10. This composite diagram illustrates the inferred structure beneath the Chugach profile as determined from the refraction data and projects it southward based on the mapped surface geology. The relationships of structures adjacent to the Contact fault system are not clear. On the surface, the Contact Fault appears to mark a major suture zone which separates two geologically different areas [Winkler and Plafker, 1981]. We present in Figure 10 the interpretation that sediments have been accreted to and thrust under rocks

of the Chugach terrane. Lower layers are presented as rocks which lack surface expression and do not extend southward beyond the Contact fault zone [Fuis and Ambos, 1986]. These lower layers have velocities compatible with those found for oceanic crust, and it is suggested that they comprise different layers of an underthrust subduction package. Earthquake focal depths are believed to delineate the top of the current subducting plate at approximately a 30-km depth and provide a lower limit to the upper crustal package (Figure 10). The refraction data lack evidence of a sharp velocity contrast at this depth, a finding which suggests that the bottom of the overriding crust and the top of the subducting plate may have similar composition. Refraction data alone are insufficient to uniquely determine the complex geometries and relationships of deep structure beneath 22 km, between the accreted Chugach and Prince William terranes and the subducting plate.

2.7 Acknowledgments.

the geologic and tectonic interpretation, and L. Braille and R. Keller for their critical review.

CHAPTER 3: CORDOVA PEAK SEISMIC REFRACTION PROFILE[2]

3.1 Introduction.

Southern Alaska is a geologically and tectonically complex area which offers a

modern setting for the study of subduction environments and accretionary processes

(Figure 1). It consists of a collection of tectonostratigraphic terranes which were

accreted to the North American continent along a convergent margin. A recent

contribution towards our understanding of the tectonic processes and geologic history

of southern Alaska has come from data collected as part of the U.S. Geological

Survey's Trans-Alaska Crustal Transect (TACT) project, an ongoing program of

geological and crustal seismic investigations. In this paper, a three-dimensional crustal

model for a part of southern Alaska is developed from an interpretation of two

intersecting TACT seismic refraction profiles, the Chugach and the Cordova Peak

profiles. A detailed model based on the Chugach profile was developed in a previously

published study [Wolf and Levander, 1989] and is incorporated into the Cordova Peak

model developed in this paper.

---

[2]Chapter 3 contains the text of a manuscript entitled, *Upper Crustal Structure of
Southcentral Alaska: An Interpretation of TACT Seismic Refraction Data* to be
submitted to the *Journal of Geophysical Research*. To avoid repetition, the reader
may wish to proceed to the Data and Analysis section (3.3).

45

The 126-km Cordova Peak seismic refraction line is a N-S trending dip profile which crosses both the Chugach and Prince William terranes. At its midpoint, the Cordova Peak line intersects the Chugach line, a 135-km profile which parallels the regional E-W strike of structures in the Chugach Mountains (Figure 2). The Chugach and Prince William terranes form an accretionary complex divided by the Contact fault zone, a zone of steeply dipping faults along which rocks of the Prince William terrane have been thrust beneath older rocks of the Chugach terrane. In the western part of the Gulf of Alaska, the Aleutian trench forms the southern boundary of the Prince William terrane, separating it from the subducting Pacific plate. In the central Gulf region, the eastern boundary of the Prince William terrane is a fault contact with the Yakutat terrane along the Kayak Zone.

3.2 Regional and tectonic setting.

Southern Alaska has been divided into tectonostratigraphic terranes which represent distinct, fault-bounded geologic entities with different geologic histories [Jones et al., 1981; 1987; Howell et al., 1985; Stone and Wallace, 1987]. The Chugach, Prince William and Yakutat terranes are three such entities which lie north of the Gulf of Alaska (Figures 1 and 2). The TACT corridor is located in a transitional area influenced by both convergent and transform tectonic margins. To the west, the Pacific plate is subducting beneath the North American plate, beginning along the

Aleutian trench. To the east, transform motion is distributed along the Fairweather

fault system.

3.2.1 Plate interactions.

Relative motion between the Pacific and the North American plates was described

by the RM1 model [Minster et al., 1974] to be approximately NNW at a rate of 6

cm/yr, an estimate which is in agreement with more recent models for this region

[Engebretson et al., 1985]. Within this transition zone between convergent and

transform margins, motion cannot be accomodated entirely by a well-defined

boundary, as indicated by new or reactivated faults and by internal deformation of

inland continental rocks [Perez and Jacob, 1980; Jacob, 1986; Lahr and Plafker, 1980].

Estimates of convergence rates and paleolatitudes suggest that the terranes in southern

Alaska contain rocks that were originally deposited south of their present latitudes and

later travelled northward as the result of plate motions [Stone and Panuska, 1982; von

Huene et al., 1985]. They were then accreted to and/or subducted beneath southern

Alaska along the Gulf of Alaska margin.

3.2.2 Terrane descriptions.

The Chugach terrane consists of highly deformed, accreted and metamorphosed

clastic sedimentary rocks and oceanic crust [Winkler et al., 1981]. It has been divided,

from north to south, into three major fault-bounded sequences: the Upper Jurassic or older Liberty Creek schists, the Jurassic or older to Lower Cretaceous McHugh Complex and the Upper Cretaceous Valdez Group [Winkler et al., 1981; Silberling and Jones, 1984; Plafker et al., 1989].

The Valdez Group, which forms the bulk of the Chugach terrane, consists mainly of continentally-derived sediments which were eroded from a magmatic arc and deposited in a deep-sea fan [Winkler et al., 1981; Plafker et al., 1989]. Beneath the deposited sedimentary rocks, mafic volcanic oceanic rocks form the terrane basement [Winkler et al., 1981]. The Chugach terrane moved northward to its present location, forming a thick accretionary prism which was progressively deformed and metamorphosed in a low pressure/high temperature event beginning in latest Cretaceous and continuing in Paleogene time [Hudson and Plafker, 1982].

An observed metamorphic gradient in Valdez Group rocks increases from greenschist facies in the west to amphibolite facies east of the Copper River in the Chugach Metamorphic Complex [Hudson and Plafker, 1982; Sisson and Hollister, 1988]. To the south, metavolcanic rocks exposed at the surface are juxtaposed with sedimentary rocks of the Prince William terrane along the Contact fault zone. The total stratigraphic thickness of the Chugach terrane is unknown.

The Prince William terrane contains rocks of the Orca Group, a late Paleocene and Early through Middle Eocene deep-sea fan deposit interbedded with oceanic

basalts [Winkler and Plafker, 1981; Plafker, 1987]. There is evidence that these rocks were deposited south of their present latitude and were later transported northward, accreted and metamorphosed to zeolite to greenschist facies [Plafker, 1987; Plumley and Plafker, 1983; Panuska and Stone, 1985]. The Orca Group forms the basement of the Prince William terrane, with an estimated thickness of 6-10 km. Overlying the Orca Group are Late Eocene or older to Quaternary siliciclastic sedimentary rocks which were deposited in shelf or slope basins at their current locations [Plafker, 1987]. These younger sedimentary rocks constitute a relatively undeformed sequence estimated to be less than 4 km thick [Plafker, 1987].

Similarity in lithology and depositional environment between the sandstones of the Chugach and Prince William terranes has raised some question as to whether the two terranes are geologically distinct entities and properly can be called terranes [Dumoulin, 1988]. In the western Prince William Sound, little metamorphism or deformation is observed in these terranes and no well defined compositional boundary exists at the Contact fault zone [Dumoulin, 1988]. Because of this similarity, it has been argued that the minor differences seen in rocks of the two terranes in central Prince William Sound may simply reflect a metamorphic gradient and that the Contact fault zone may be a series of thrust faults in a developing accretionary prism rather than a terrane boundary.

Felsic to intermediate Eocene hypabyssal and plutonic rocks were intruded into the Chugach and Prince William terranes at about 50 Ma ago, following the start of regional metamorphism [Plafker et al., 1989]. The intrusions form dikes and dike swarms, as well as sills and small stocks which crop out in the vicinity of the seismic transect. Crosscutting relationships indicate that intrusions post-date deposition of Orca Group rocks and major motion along the Contact Fault [Winkler and Plafker, 1981].

The Yakutat terrane is to the east of the Prince William terrane and southeast of the TACT corridor. Although rocks of the terrane are not seen along the transect, subsurface boundaries of the terrane may well extend westward to the transect and beyond. The Yakutat terrane can be subdivided into two segments: west of the Dangerous River zone, the basement is composed of Paleocene to Early Eocene oceanic crust, and to the east, the basement is composed of continentally derived upper Mesozoic flysch and melange of the Yakutat Group [Plafker, 1987]. Overlying the basement rocks are Lower Eocene to Quaternary clastic sequences, some of which are thought to be derived locally from erosion of the Chugach and St. Elias Mountains after collision and underthrusting of the Yakutat terrane [Plafker, 1987]. There is evidence that the Yakutat terrane originated to the south and travelled approximately 400-600 km northward to its present location [von Huene et al., 1985; Plafker, 1987]. Studies indicate that the Yakutat terrane is currently accreting along the Gulf of Alaska

margin. It appears to be moving with the Pacific plate but at a slightly lower rate,

which suggests that remaining motion must be accomodated by faulting or internal

deformation of the terrane [Perez and Jacob, 1980; Lahr and Plafker, 1980; Plafker,

1987; Bruns, 1983].

3.3 Data and analysis.

The N-S Cordova Peak profile extends from the Border Ranges fault zone to the

Gulf of Alaska (Figure 2). It is a reversed profile consisting of five shots, each

recorded by approximately 120 portable seismic recorders spaced at 1-km intervals in a

fixed array [Wilson et al., 1987]. Shot points 11, 12 and 19 lie within McHugh

Complex and Valdez Group rocks of the Chugach terrane. Shot points 38 and 37 lie

south of the Contact fault zone, within rocks of the Prince William terrane. Shot point

19 marks the intersection of the Cordova Peak dip line with the Chugach strike line.

3.3.1 Procedure.

The five shots of the Cordova Peak profile have been interpreted using two-

dimensional asymptotic ray tracing [Luetgert, 1987] and the standardized procedure

discussed in the Appendix. Field records indicate that the seismic data are of good

quality except at long offsets, where signal to noise ratios make it difficult to pick first

arrivals in some record sections. Calculated travel times were generally fit to within

0.05-0.10 s, except at long offsets or in areas where the ray-tracing algorithm did not permit small-scale modelling. These areas are discussed in more detail below. Synthetic seismograms produced using the program R86PLT [Leutgert, 1987] were used to match amplitudes in the observed data and to refine the velocity structure within the model.

Results of the modelling are shown in Figures 11-15. Each figure contains a comparison of the field data from one shot point with the calculated travel times and synthetic seismograms from the preferred model. Record sections are plotted with a reduction velocity of 6 km/s and are trace normalized. Ray diagrams illustrate the subsurface areas sampled in different layers, but for simplification, only representative rays are shown. Sea level corresponds to a depth of 2 km in the model. Simplified topography is drawn from local maxima and minima as determined from receiver elevations [Wilson et al., 1987].

The starting model for the Cordova Peak interpretation was constructed from a synthesis of one-dimensional models from each of the shot points, a model based on surface geology and geologic cross-sections, and the previously derived model for the intersecting Chugach line (Figure 9) [Wolf and Levander, 1989]. The starting model was then iteratively adjusted and revised. Several assumptions made in these initial attempts at matching travel times and phases yielded poor results. For instance, it was difficult to constrain rigorously the Cordova Peak dip model at shot point 19 (the
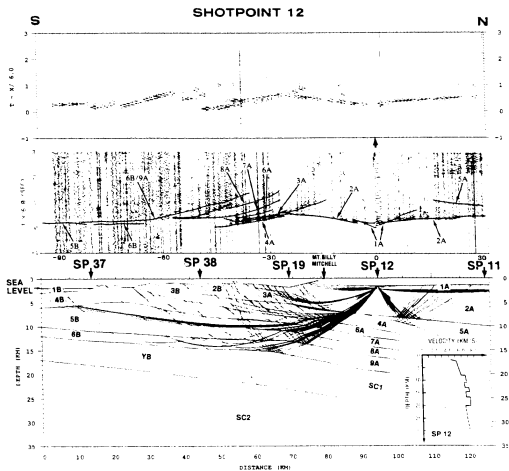
Figure 12. Reduced-time record section with calculated travel time curves, synthetic record section and ray diagram for shot point 12 (SP 12). Calculated travel times from same branch are connected and overlie trace-normalized record section. Velocities given in kilometers per second. Some curves are omitted to avoid clutter in the diagram. Amplitudes for offsets beyond 60 km are not well constrained because of limited accuracy at long offsets (see text).
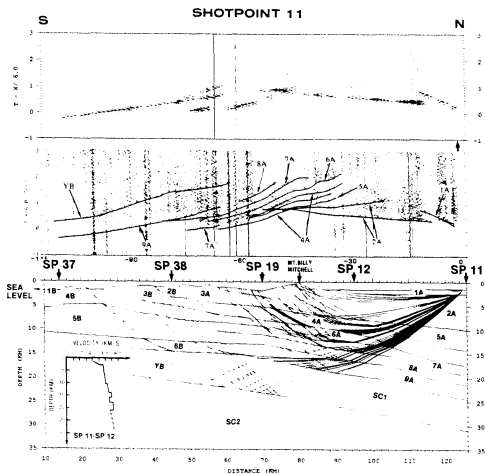
Figure 11. Reduced-time record section with calculated travel time curves, synthetic record section and ray diagram for shot point 11 (SP11). Calculated travel times from same branch are connected and overlie trace-normalized record section. Velocities given in kilometers per second. Some curves are omitted to avoid clutter in the diagram. Amplitudes for offsets beyond 60 km are not well constrained because of limited accuracy at long offsets (see text).
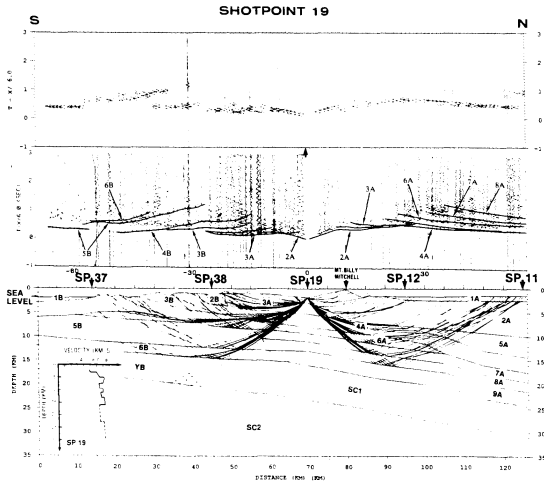
Figure 13. Reduced-time record section with calculated travel time curves, synthetic record section and ray diagram for shot point 19 (SP 19). Calculated travel times from same branch are connected and overlie trace-normalized record section. Velocities given in kilometers per second. Some curves are omitted to avoid clutter in the diagram. Amplitudes for offsets beyond 60 km are not well constrained because of limited accuracy at long offsets (see text).
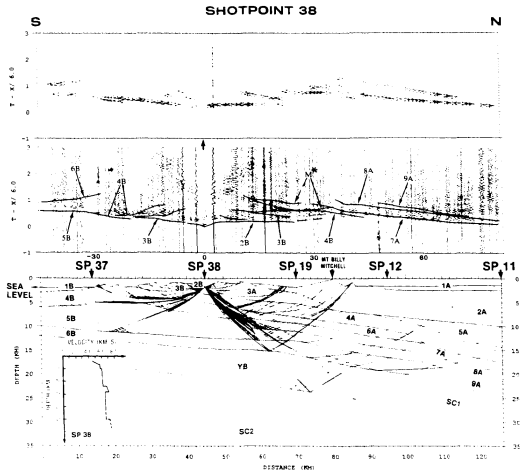
Figure 14. Reduced-time record section with calculated travel time curves, synthetic record section and ray diagram for shot point 38 (SP 38). Calculated travel times from same branch are connected and overlie trace-normalized record section. Velocities given in kilometers per second. Some curves are omitted to avoid clutter in the diagram. Amplitudes for offsets beyond 60 km are not well constrained because of limited accuracy at long offsets (see text). M* indicates travel time curves for surface multiples.
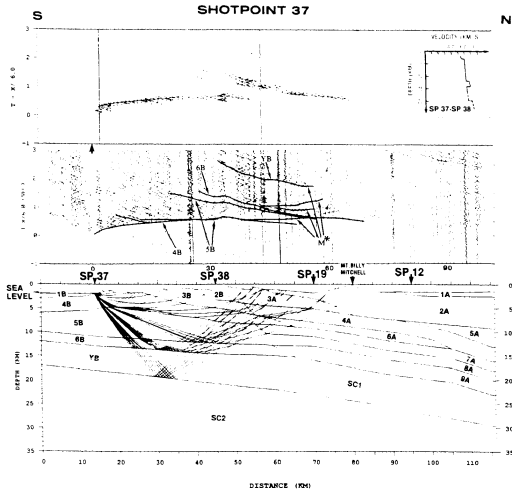
Figure 15. Reduced-time record section with calculated travel time curves, synthetic record section and ray diagram for SP 37. Calculated travel times from same branch are connected and overlie trace-normalized record section. Velocities given in kilometers per second. Arrivals from surface multiples are marked with asterisks. Some curves are omitted to avoid clutter in the diagram. Amplitudes for offsets beyond 60 km are not well constrained because of limited accuracy at long offsets (see text). M* indicates travel time curves for surface multiples.

intersecting point of the two lines) with the velocity-depth function from shot point 19 in the Chugach model. Velocities of the strike line were systematically too high to match travel times in the dip line, unless a fairly significant lateral velocity gradient was invoked. Once the constraint from the velocities observed in the strike direction was relaxed, model adjustments met with more success. At least two possible explanations can be presented for the velocity-depth function discrepancies between the strike and dip models. First, energy recorded along the strike direction could represent rays travelling out-of-the-plane of section. Secondly, velocity-depth discrepancies could reflect anisotropy in rock properties. This second possibility is discussed in more detail below.

A second assumption made in the starting model was that units appearing at the surface in the Prince William terrane could be projected downdip to the north in the model, beneath the Chugach terrane. Attempts to follow this approach required unreasonable velocity increases from south to north within the layers. For instance, an attempt to carry layer 3B downdip to the north required an increase in average velocity from 5.6 km/s to 6.7 km/s (Figure 16). This steep gradient is more likely to indicate a compositional change than a change due to an increase in velocity with depth or metamorphic grade.

Figure 16. Seismic model showing average velocities, gravity and magnetic data, and possible geologic structure based on seismic refraction interpretation of USGS Cordova Peak profile: (a) Gravity from Barnes [1977] and D.F. Barnes [written commun.,1984]; magnetic profile modified from Page et al. [1986], Andreason et al. [1964] and U.S. Geological Survey [1979a, 1979b]. (b) Velocity model showing average velocities for model layers; shaded portion denotes areas sampled by rays from reversed shots. Velocities and boundaries outside shading are not well constrained. (c) Possible geologic interpretation based on seismic model and cross section from G. Plafker et al.[1989].

CORDOVA PEAK MODEL

S · N

(a)

GRAVITY (MGALS)

MAGNETICS (NT)

+80 · +60 · +40 · +20 · 0 · -200

MAGNETICS
GRAVITY

GRAVITY FROM BARNES, 1977; PAGE ET AL., 1986
MAGNETICS FROM PAGE ET AL., 1986; ANDREASON ET AL., 1964; USGS, 1979

0   10   20   30   40   50   60   70   80   90   100   110   120

DEPTH (KM)

3.7 1B   2B 3A
     4B 5.4 3B 5.6 5.2   8.1   5.8   1A 4B
     5B 6.2   5.6 5.8 6.0   6.9 4A   5.8   2A
     6B   6.8   6.0   8.5 6A   6.7   6.0 5A
          6.5?   7.0   6.4
                        YB   7.0   7A
                                   7.2   8A
                                        ?   7.2?   8A
                                                                  SC1
                              SC2

(b)

DISTANCE (KM)

SP 37   PWT   SP 38   SP 19 MT BILLY   SP 12   CGT   SP 11
                    CFZ   MITCHELL

SEA
LEVEL

ACCRETIONARY   SEDIMENTS   MAFIC VOLCANICS   METAMORPHOSED FLYSCH
                    FELSIC INTRUSIVES   MAFIC TO ULTRAMAFIC ROCKS   FELSIC ?
PWT ACCRETED SEDIMENTS   ?   LVZ   INTRUSIVES
PWT BASEMENT? (MAFIC TO ULTRAMAFIC)   MVZ   ?
     ?   LVZ
              YAKUTAT TERRANE   (LVZ) MVZ   RELICT SUBDUCTED
                                               OCEANIC CRUST?
                                          ?   SUBDUCTED OCEANIC CRUST?
              SUBDUCTED OCEANIC CRUST?

(c)

0   10   20   30   40   50   60   70   80   90   100   110   120

DISTANCE (KM)

3.3.2 <u>Seismic model</u>.

The seismic velocity model derived for the Cordova Peak profile is shown with observed gravity and magnetic data and a possible geologic model in Figure 16 a-c. The seismic model consists of 18 layers, each displayed with average compressional velocities for specific areas in the model. The upper layers are grouped according to terrane, with layers 1A-5A corresponding to rocks of the Chugach terrane, and layers 1B-6B corresponding to rocks of the Prince William terrane. Mid-crustal and deeper layers are treated separately. Table 1 contains a summary of layer information, listing layer thicknesses, velocity ranges and depth ranges.

3.3.2-1 Chugach terrane.

Layers 1A-5A represent rocks of the Chugach terrane, most of which have surface expression north of the Contact fault zone [Winkler et al., 1981]. Compressional velocities at the surface in the Chugach terrane range from average lows of 4.0 km/s to average highs of 5.8 km/s in exposed bedrock. Clearly observed primary arrivals and prominent reflections generally provide good constraints on depths to interfaces of the first four layers (Figures 11, 12 and 13). A comparison of arrivals at offsets within 20 km to the north and south in the record from shot point 19 indicates a change in the near-surface structure and a steepening of the northward dip (Figure 13). The record section exhibits clear first arrivals and little complication at offsets within 20 km north

TABLE 1: CORDOVA PEAK MODEL

Chugach terrane LAYER	AVERAGE STRUCTURAL THICKNESS (KM)	VELOCITY RANGE (KM/S)	AVERAGE VELOCITY (KM/S)	GEOLOGIC INTERPRETATION
1A	1	4.00-5.15	4.5	Unconsolidated sediment
2A	6	4.73-5.90	5.7	Metamorphosed flysch
3A	3	5.80-6.40	6.2	Mafic metavolcanics
4A	2	6.40-7.40	6.9	Mafic to ultramafic metavolcanics
5A	3	5.90-6.10	6.0	Metamorphosed flysch and igneous intrusive rock
Mid-crustal layers				
LVZ 1	2	6.40-6.50	6.5	Underplated oceanic sediments or zones of high porosities
HVZ 1	2	6.85-7.00	6.9	Mafic to ultramafic oceanic crust
LVZ 2	2	6.60-6.70	6.6	Mafic oceanic crust
HVZ 2	3	7.10-7.25	7.2	Mafic to ultramafic oceanic crust
Prince William terrane				
1B	1	3.70-3.75	3.7	Unconsolidated sediments
2B	2	4.50-5.40	5.2	Metasedimentary rocks
3B	3	5.60-5.70	5.7	Metasedimentary rocks
4B	3	5.00-6.10	5.6	Sedimentary, metasedimentary and igneous intrusive rocks
5B	6	6.10-6.30	6.2	interbedded metasedimentary and volcanic rocks
6B	2	6.70-7.00	6.9	Mafic to ultramafic volcanic rocks
Deep crustal layers				
YB	6?	6.40-6.80	6.5	Terrigenous sedimentary rocks overlying oceanic crust
SC1	6?	6.60-7.20	7.0	Mafic to ultramafic oceanic crust
SC2	?	7.05-7.25	7.2	Mafic to ultramafic oceanic crust

61

of shot point 19. No high-amplitude reflection occurs until approximately a 23-km

offset and 0.75 s. To the south, wide-angle reflections from shallow layers occur much

closer to the shot point and contribute to complication in the waveforms. The

difference in observations of energy travelling northward versus southward from shot

point 19 is attributed to an increase in thickness of the second layer and to the pinch

out of layer 3A (Figure 13).

Layer 3A, exposed at the surface just north of the Contact fault zone, has high

average velocities (6.2 km/s) which cannot be continued northward much beyond shot

point 19 in the model. Attempts to carry this layer northward over the length of the

profile without invoking a substantial lateral velocity gradient resulted in travel times

greater than 0.25 s too fast for refracted rays within the layer. As an alternative, the

thickness of layer 2A was increased to the north; this approach provided a more

successful match not only to travel times but also to amplitudes.

Slower apparent velocities observed in all shot records in the area beneath Mt.

Billy Mitchell provide evidence of a low-velocity area in layer 2A, located at 80-90 km

from the south end of the model (Figure 16). In the data from shot point 11, a delay in

the travel time curve is seen at approximately 40-50 km offset (Figure 11). A similar

delay is seen in the record southward from shot point 12 at approximately 15-20 km

offset (Figure 12). Because it is observed in the same location even from shots at far

offsets, the delay is associated with a near-surface feature in layer 2A (Figures 14 and

15). Coincident with the travel time anomaly is a loss of high frequency energy in the area near Mt. Billy Mitchell (Figures 11 and 13). The combination of these two attributes in the same location indicates that some structural complexity, such as a fault, may exist in this area.

Although layers 4A and 5A do not extend to the surface, they have been grouped with units associated with the Chugach terrane in the model. The primary rationale for grouping these layers with layers 1A-3A above comes from seismic reflection data collected in the northern portion of the model [Fischer et al., 1989]. A clear difference in the character of signal is seen in the reflection data between the upper crust and mid-crustal layers (Figure 17). The data show that the upper 10 km of crust of the Chugach terrane contains several discontinuous reflections with various orientations, while layers below approximately 10-12 km have prominent, more continuous reflections [Fischer et al., 1989].

In the record from shot point 12, a clear wide-angle reflection at a 17-km offset to the south indicates the location of the interface between layers 2A and 4A (Figure 12). To the north, the shot record lacks such a strong arrival, evidence which may suggest a smaller velocity contrast between layer 2A and the unit below. Layer 5A was introduced to the model to accomodate differences seen to the north and south in the shot record. Velocities near the top of layer 5A are similar to those in the layer above,
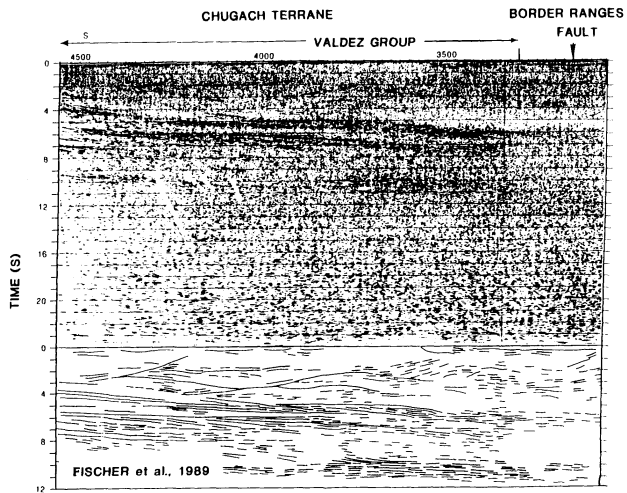
Figure 17. Modified figure showing data from TACT Chugach seismic reflection profile [Fischer et al., 1989]. Mid-crustal layers show prominent, continuous reflections, whereas crust imaged above 4-6 seconds in the data does not.

an observation which is supported by a lack of a distinct, continuous high-amplitude wide-angle reflection at near offsets in the data from shot point 11 (Figure 11).

Observed travel times of rays refracted to the south of shot point 19 at offsets of 20 km and 0.0 s in the field data are slightly faster than those calculated from the model (Figure 13). A similar discrepancy appeared in the comparison of calculated and observed travel times from SP19 in the Chugach data at offsets of 40 km (Figure 5). These early primary arrivals are attributed in both cases to refracted rays which cross lens-shaped high-velocity areas (7.4 km/s) in layer 4A in the Cordova Peak model (layer 3 in the Chugach model). Because no discrepancy in the travel times occurs to the north of shot point 19, the high-velocity areas are assumed to pinch out. A discussion on the modelling of these lenses appears in the paper on the Chugach profile [Wolf and Levander, 1989].

3.3.2-2 Mid-crustal layers.

The group of mid-crustal rocks containing low/high velocity pairs begins at approximately 8 km beneath shot point 19 in the model (Figure 16). The model contains two low-velocity layers, the first of which has an average velocity of 6.5 km/s and is shown to pinch out at approximately 35 km to the north of shot point 19 in the Cordova Peak model (and 30 km to the east in the Chugach model (Figure 9)). Directly beneath the first velocity reversal is a sharp increase in average velocity to 6.9

km/s, corresponding to a high-velocity layer. The second low-velocity layer, occurring at about 10-12 km depth in the model, has an average velocity of 6.6 km/s and is shown to be thicker and more homogeneous than the first. It is again followed by a high-velocity layer, having an average velocity of 7.2 km/s. The low-velocity zones are indicated in the refraction data by high-amplitude second arrivals (thought to result from energy reflecting from the base of the low-velocity layers), complication in the record section, and delays or skips in the travel time curves. En echelon arrivals are especially apparent in the refraction data from the Chugach strike line and are discussed in detail in that analysis (Figures 3-6) [Wolf and Levander, 1989].

Energy arriving beyond an offset of 25 km to the north in the record from shot point 19 is similar in character to that arriving at offsets of 10-25 km to the south (Figure 13). In both directions, high-amplitude secondary arrivals are attributed to impedance contrasts between low- and high-velocity layers and to the almost coincident arrival of reflections from the base of the low-velocity layers (6A and 8A) with refracted energy from the high-velocity layers (7A and 9A) below (Figure 13). In the record from shot point 11, for instance, complication and numerous high-amplitude arrivals as well as increased velocities are observed beyond an offset of 45 km, as rays pass through crust containing the velocity reversals and high-velocity layers.

Distinct horizons appearing in the Chugach seismic reflection data were used in the refraction model to provide some constraint on the depths to interfaces of these

low-/high-velocity layers, since they cannot be well modelled from refraction information alone (Figure 17). The reflection data were also used to provide information on the continuity of layers at the model's northern boundary, since mid-crustal and deeper layers there lack reversed ray coverage; the subsurface area along the profile actually sampled by the rays from reversed shots is shown by shading in Figure 16.

A preliminary model of the Chugach line used four low-/high-velocity pairs to match en echelon arrivals observed in the data [Fuis and Ambos, 1986; Page et al., 1986]. This model resulted in primary arrivals from the higher velocity layers occurring at distances not seen in the field data. A more successful approach was to model en echelon arrivals in the data from the Chugach strike profile as multiple reflections within the second low-velocity zone using reflectivity methods [Flueh et al., in preparation]. Although the reflectivity method is more exact, it is also considerably more computationally expensive. Results of modelling multiples using the ray series approximation are displayed and discussed in more detail in the interpretation of the Chugach strike line [Wolf and Levander, 1989].

3.3.2-3 Prince William terrane.

The velocity of surface layers in the Prince William terrane range from average lows of 3.7 km/s to average highs of 5.6 km/s (Figure 16). Layer 1B, used to represent

surficial deposits in the shoreline area south of shot point 37, thickens southward near the model boundary. This end of the profile does not have reversed coverage and has not been well modelled. The Contact fault zone is modelled as a wedge (layer 2B) in an attempt to represent a system of faults. Its average velocity is 5.2 km/s. The wedge boundaries correlate with the mapped positions of the Rude River and Gravina faults, thought to be splays of the Contact Fault [Winkler and Plafker, 1981]. A maximum delay in arrivals of approximately 0.25 s and a loss in high-frequency energy are seen in all shot records in the area of the Contact fault zone (Figures 11-15).

Layer 3B and a portion of layer 4B (about 30 km from the south end of the model) are shown to have average velocities of 5.6 km/s. Although these two layers are modelled as separate units, a similarity in their respective velocities indicates that they may represent duplicated sections of the same rock type (Figure 16). The proximity of the fault zone and intrusive rocks make it difficult to identify phases in arriving energy and therefore the geometry of layers in this area of the model is not well constrained. A slight delay occurs in primary arrivals approximately 17 km south of shot point 38 (Figure 14). This travel time delay may provide evidence of a structural feature, possibly a fault, which could produce a duplication of section. Downdip to the north and below layer 3B (30-60 km from the south end of the model), the average velocity of layer 4B increases from 5.6 to 6.0 km/s (Figure 16). A larger velocity contrast between layer 3B and 4B in this area of the model is suggested in the data from shot

point 38, where a clear reflection is observed at 10-15 km offset to the south (Figure 14). This lateral increase in velocity is believed to represent a lithological change rather than a change due to increasing depth or degree of metamorphism because the gradient is steep. Layers 3B and 4B are shown to terminate at or near the Contact fault zone in the model. As discussed earlier, attempts to project these units northward required an unrealistic velocity gradient (see 3.3.1).

Primary arrivals from shot point 38, which is located within the wedge (layer 2A) in the model, are fairly symmetric within 15 km of the shot point (Figure 14). Since the structure is assumed to be north-dipping on the basis of geologic data [Plafker et al., 1986], a similarity in apparent velocity of rocks to the north would represent higher velocity material than that to the south. On a broader scale, the significant decrease in velocities within Prince William terrane rocks as compared with those within the Chugach terrane at comparable depths is clearly evidenced in the shot records. In the data from shot point 12, for instance, the slopes of primary arrivals decrease as energy passes from the Chugach terrane into the Prince William terrane, as seen at offsets beyond 60 km (Figure 12).

Layer 5B and 6B do not appear at the surface in the model. They are grouped with rocks of the Prince William terrane on the basis that they represent units which appear on the surface to the south and agree with geologic estimates of thickness (see 1.1.2) [Plafker, 1987]. Layer 5B is a thick, homogeneous unit having an average

velocity of 6.2 km/s and a small vertical velocity gradient (Figure 16b and Table 1). It is underlain by a thinner layer having average velocities of 6.9 km/s and a much steeper vertical gradient.

Evidence for the velocities and geometries of layers 5B and 6B is best seen in the field data from shot point 37 (Figure 15). This shot record is significantly different from other shot records of the Cordova Peak profile. It is characterized by clear, obvious arrivals with few complications. A high-amplitude second arrival is observed at approximately a 33-km offset and 0.6 s. This secondary pulse is associated with refacted energy arriving from layer 6B, almost coincidently with strong reflections from the base of layer 5B.

3.3.2-4 Deep structure.

The velocity structure of deeper layers beneath the Chugach and Prince William terranes is not well constrained. Layer YB is shown to terminate at a boundary with SC1 at about 90 km from the south end of the model (Figure 16). Several assumptions were made in dividing this area of the model into two units with significantly different average velocities (6.5 km/s for YB and 7.0 km/s for SC1). As mentioned previously, the geometry and velocities of deeper layers in the northern part of the profile are outside the region of reversed shot coverage. Layer interfaces and velocities for this area are based on the northward continuation of layers in the model's central portion

and on locations indicated by interpretations of other data to the north [Fuis et al., in preparation; Fischer et al., 1989]. Velocity-depth functions from Fuis et al. [in preparation] indicate average velocities from 7.0-7.5 km/s for depth ranges corresponding to layers YB and SC1. These are averaged in layer SC1 to 7.0 km/s. Smoothed versions of the velocity functions used by Fuis et al. are incorporated into the processing of reflection data to the north [Fischer et al., 1989]. Primary arrivals in the Cordova Peak profile at offsets beyond 100 km, however, indicate average velocities of about 6.4-6.5 km/s (Figures 11 and 15). The deep areas sampled by these rays are between 50-80 km from the south end of the model (Figure 16). These two somewhat conflicting estimates of the velocities associated with layers YB and SC1 can be accomodated by introducing a boundary into the model at the location shown by the hatched area in Figure 16. Since a precise location for such a boundary cannot be determined from the data, it is represented in the model by a lateral velocity gradient.

There is little evidence in the refraction data for the top interface of layer SC2. Evidence for a boundary at this location comes primarily from earthquake data and seismic reflection data. Earthquake hypocenters for events located within the subducting plate can be traced northward from the Aleutian trench to approximately this depth along the profile direction [Davies, 1975; Lahr, 1975; Stephens et al., 1984; Page et al., in preparation]. These hypocenters were used to provide a lower limit for the overriding crust [Wolf and Levander, 1989]. In the reflection data acquired along

the northern section of the Cordova Peak line, a prominent reflection which might be correlated with the top of the subducting plate is observed at a depth approximately corresponding to the top of SC2 in the model [Fischer et al., 1989]. On the basis of these two data sets, layer SC2 was included in the refraction model. The lack of a prominent arrival could be the result of a low impedance contrast in some areas of the profile or of high noise levels in the data at far offsets.

An interesting feature in the record from shot point 37 is the longer period and associated delay of both primary and secondary arrivals seen in the vicinity of Mt. Billy Mitchell. Since these arrivals occur at similar offsets (60-70 km) but significantly different times (0.6 s and 0.8 s), they have been modelled as multiple reflections within the near surface layer south of the topographic high. Multiple reflections for the later arrival correspond in travel time to reflections from the base of YB which are again reflected at the surface. Although a somewhat successful match to travel times of these arrivals was made, attempts to match amplitudes in this area of the model and at far offsets were not successful. Amplitudes produced by the synthetic seismogram algorithm are extremely sensitive to complex structures which exist in the region of the terrane boundary; therefore very slight changes in boundary geometries produce dramatically different results. (See earlier discussion on Figure 8.)

At approximately a 75-km offset and 3.0 s in the record from shot point 37, a high-amplitude phase is observed (Figure 15). In the shot record from shot point 11, a

similar phase is observed at approximately a 90-km offset and 3.0 s (Figure 11). Although these phases have not been modelled, they are roughly correlative in time to refracted waves in layer SC2 which reflect off the surface to form multiple arrivals. Another possibility is that they represent converted phases at the SC2 boundary. By reciprocity, these two arrivals can be associated with rays sampling the same layer in the model.

3.4 Geologic interpretation.

A possible geologic interpretation with a detailed velocity model of the upper crustal structure along the Cordova Peak refraction profile is shown in Figure 16. Low velocities in the near-surface (layers 1A and 1B) are associated with alluvial sediments in river valleys and with glacial sediments which form a thin cover over rocks with much higher velocities. Rocks along the length of the profile in the Chugach terrane have been mapped as belonging to the McHugh Complex and Valdez Group. These consist primarily of metamorphosed flysch overlying mafic oceanic crust [Winkler et al., 1981]. Rocks along the profile in the Prince William terrane have been mapped as Orca Group rocks, consisting of interbedded metasedimentary and metavolcanic rocks, which are overlain by late Eocene to Quaternary clastic sedimentary rocks [Winkler and Plafker, 1981]. The geologic model represents an attempt to correlate layers in the seismic model with mapped geology.

3.4.1 Chugach terrane.

Layers 1A-5A are correlated primarily with metamorphosed flysch and volcanic rocks of the Valdez Group. Rocks of the McHugh Complex probably occur near the north end of the profile but are covered by surficial deposits [Winkler et al., 1981]. Complication in the record from shot point 11 close to the shot point may represent a subsurface contact between rocks of the Valdez Group and McHugh Complex or may be the result of diffracted or scattered energy from dikes which have intruded nearby areas of the transect [Winkler et al., 1981; Plafker et al., 1989]. Travel times in the shot record are difficult to match in this area and require substantial lateral velocity variation from shot point 11 southward (Figure 11). The dikes may contribute to higher average velocities in the northern portion of layer 2A, but are too small to be modelled as separate units. Another geologic feature which may contribute to the complicated arrival pattern and average increase in near-surface velocities is the rootless Haley Creek terrane, a thin sliver of metasedimentary and metavolcanic rocks which has been thrust over Chugach terrane rocks in this area of the transect [Wallace, 1985; Plafker et al., 1989; Nokleberg et al., 1989]. Advanced travel times indicated by primary arrivals at offsets of 10-30 km from shotpoint 11 are attributed to energy travelling through this piece of the Haley Creek terrane (Figure 11). Shot spacing and receiver density make detailed modelling of the structural relationships between rocks

of the Haley Creek terrane and those of the Chugach terrane difficult because the features are too small.

Long crossover distances and a lack of an early prominent reflection from the base of layer 2A in the records from shot point 11 and 12 provide evidence of the layer's thickness. The change in thickness from shot point 19 to shot point 11 is in part due to the northward dip, but may also be due to imbrication and thrust faulting within the accretionary complex. Further evidence of faulting within layer 2A is provided by travel time delays seen beneath Mt. Billy Mitchell.

Layer 5A is interpreted to be a downward continuation of the metamorphosed flysch in layer 2A. The lack of a strong continuous reflection in the data until about a 32-km offset from shot point 11 indicates a low impedance contrast between these two layers and raises the possibility that they are compositionally similar (Figure 11). The geometry of layer 5A suggests it may represent a thickening of the flysch sequence, possibly containing intrusive rocks. Felsic to intermediate Eocene hypabyssal and plutonic rocks, in the form of dikes , sills and small plutons, have been observed in the vicinity of the transect throughout both the Chugach and Prince William terranes [Winkler et al., 1981; Winkler and Plafker, 1981; Plafker et al., 1989]. Absence of a continuous secondary arrival in the data from shot points 11 and 12 may be in part the result of scattered and diffracted energy from these intrusions.

Layer 3A to the south corresponds to an elongate outcrop belt of mafic volcanic rocks just north of the Contact fault zone (Figure 2). High velocities thought to be associated with these rocks were also seen in the Chugach seismic refraction data [Wolf et al., 1986; Wolf and Levander, 1989]. This volcanic unit makes a good marker for subsurface structure, because it produces prominent reflections and clear refracted arrivals in the seismic data. The change in the velocity-depth function between shot point 19 and shot points 11 and 12 requires that layer 3A, with its high velocities, pinch out to the north (Figure 18).

The preferred interpretation of layer 4A is that it represents a continuation of metavolcanic rocks associated with layer 3A. Mafic volcanic oceanic crust is seen at the base of the Chugach terrane and, assuming an increase in velocity with depth, layer 4A could represent a continuation of layer 3A above or a deeper, mafic to ultramafic portion of oceanic crust. Lateral velocity variations within the fourth layer could be attributed to structural deformation from imbrication and/or compositonal layering of mafic to ultramafic rocks within the oceanic crust.

3.4.2 Mid-crustal layers.

Layers beneath the third are difficult to interpret because they are not seen in the mapped surface geology. Possible geologic interpretations have been discussed in the analysis of the Chugach strike profile [Wolf and Levander, 1989]. The dip profile in
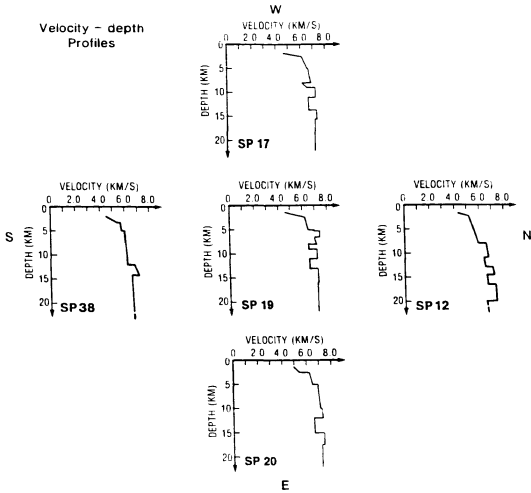
Figure 18. Velocity-depth functions shown for locations along the Chugach and Cordova Peak seismic refraction profiles. Near-surface rocks have highest velocities near SP 20, located in the Chugach Metamorphic Complex. In general, velocities are highest near SP 19. Average velocities of rocks in the Prince William terrane are lower at comparable depths to those in the Chugach terrane and provide evidence for a terrane boundary that extends to at least 10-12 km. Velocities and thicknesses of low-velocity zones are not well constrained.

the Chugach terrane does not provide information which would clearly eliminate any of the possibilities discussed. The preferred interpretation of the data is that there exist at least two low-velocity zones in the Chugach terrane: one which pinches out both to the north and to the east and a deeper one which appears to be thicker and more laterally homogeneous (layers 4 and 6 in Figure 9; layers 6A and 8A in Figure 16). Low velocities could represent subducted oceanic or terrigenous clastic sediments in which variable porosity contributes to lateral and vertical velocity variations. High-velocity layers, which underlie the low-velocity zones, are thought to consist of mafic to ultramafic rocks, possibly comprising relict subducted oceanic crust.

3.4.3 Prince William terrane.

The Cordova Peak dip profile provides valuable insight into the subsurface structure of the Prince William terrane. Lateral variations in velocity within the upper 5 km of crust provide evidence for faulting, which may be associated with imbrication of accretionary sedimentary rocks. An increase in velocity towards the north in layer 4B may be attributed to felsic intrusions near the fault zone. Although not observed at the surface directly along the refraction line, felsic sills and plutons are seen nearby [Winkler and Plafker, 1981; Plafker et al., 1986]. From a depth of 5 to 10 km, vertical velocities in layer 5B vary little. Layer 5B has velocities (6.2 km/s) consistent with those of sedimentary rocks which may have been metamorphosed. A sharp increase in

velocities and a high-amplitude reflected phase suggest a lithologic change beneath layer 5B. Mafic volcanic rocks, mainly basalts, have been observed in the Prince William terrane to the south of the transect and may project northward to occur at approximately this depth along the transect [Winkler and Plafker, 1981]. These mafic rocks in contact with sedimentary rocks could provide an impedance contrast which would account for the high-amplitude secondary arrivals seen in the data (Figure 15). Layers 5B and 6B are correlated with rocks of the Orca Group, which have thicknesses compatible with those estimated from the mapped geology [Winkler and Plafker, 1981; Plafker, 1987]. Layers 1B-4B are also in agreement with thickness estimates for sedimentary rocks which overlie the Orca Group [Plafker, 1987].

3.4.4 Contact fault zone.

The seismic refraction data do not provide good constraints on the subsurface location of the Contact fault zone, except where shots are located nearby. The location and attitude of the fault are even less discernable with increasing depth, as resolution decreases. The best-fit model shown in Figure 16 is the result of iterative trials of over 15 different configurations of the Contact fault zone. Based on geologic investigations [Winkler and Plafker, 1981; Plafker et al., 1986], potential field data (discussed below) and the best-fit seismic model, the Contact fault system is shown as having moderate northward dips (approximately 45 degrees). Layer 4B in the model appears to crosscut

the fault zone and may represent intrusive igneous rock. This crosscutting relationship

has been observed at the surface along the Contact fault zone [Plafker et al., 1986].

Although the precise geometry and location at depth of the boundary between the

Prince William and Chugach terranes are not known, the seismic refraction data

indicate very different velocity-depth functions for the two terranes to at least a 10- to

12-km depth (Figures 18 and 19). The difference in velocities at comparable depths in

the two terranes provides evidence for a boundary which separates two distinct

geologic rock assemblages to at least a 10-km depth.

3.4.5 Deep structure.

Interpretation of the data for information on the deep structural relationships is

speculative, since the area covered by rays from reversed shots is limited (Figure 16).

A flattening of the reduced travel time curves to approximately 6.5 km/s at offsets

greater than about 50-60 km precludes the downward continuation of the high

velocities associated with mid-crustal layers (Figures 11, 12 and 13). The requirement

of a low-velocity layer (YB) at a depth of 15-20 km in the model may provide evidence

that the continental crust of the Yakutat terrane extends from its mapped surface

location in the southeast to an area along or beyond the transect line (Figures 1 and 16).
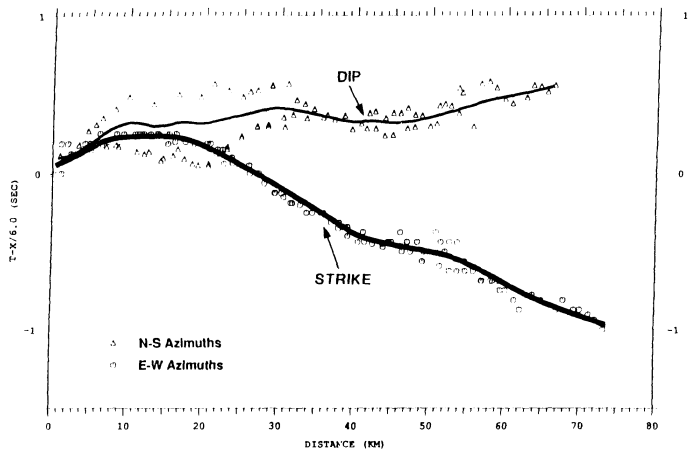
Figure 19. Observed primary arrival times from Chugach (E-W) and Cordova Peak (N-S) shot records for shot point 19.

Velocity information from interpretations of seismic reflection and refraction surveys in the northern Chugach terrane suggests that layer YB does not continue to the north of the Cordova Peak line. Layer YB is therefore shown to terminate in the northern portion of the model. One possible rationale is that this termination marks a boundary between the Yakutat terrane and relict subducted oceanic crust (layer SC1).

Layer SC2 is correlated with the subducting Pacific plate on the basis of interpretations of earthquake foci [Davies, 1975; Stephens et al., 1984; Page et al., in preparation]. Earthquake hypocenters can be traced from the Aleutian trench northward to a depth of 25-35 km beneath the Chugach Mountains. The top of layer SC2 in the model represents the approximate location of the plate interface based on the assumption that the hypocenters correspond to seismic events occurring in the upper portion of the subducting plate. There is no compelling evidence for a sharp velocity discontinuity at the depths postulated for the subducting plate based on the refraction data. For this reason, layer YB was modelled with a moderately steep vertical velocity gradient in some areas to reduce the amplitudes of reflected energy from its lower boundary. A steep vertical velocity gradient would be consistent with the composition of the western portion of the Yakutat terrane, which consists of sedimentary rocks underlain by higher velocity mafic volcanic rocks [Plafker, 1987].

3.5 Discussion of other geophysical data.

3.5.1 Gravity, magnetic and seismicity data.

Complete Bouguer gravity data are shown for southcentral Alaska in Figure 20 [Barnes, 1977]. Observed gravity and magnetic data from more recent contributions are presented in Figure 16 [Page et al., 1986]. Gravity and magnetic data provide restrictions on the crustal structure determined from seismic refraction data alone. Along the Cordova Peak line, gravity values range from a high of approximately +20 mgal (2.0 x 10^{-4} m/s^2) to a low of -80 mgal (-8.0 x 10^{-4} m/s^2) (Figure 16). A broad gravity high is located approximately 55-85 km from the south end of the model. Magnetic data along the transect also show a relative high (approximately 350 nT) just to the north of the Contact fault zone (47-55 km from the south end of the model) and a gradual northward decrease (Figure 16). Both highs correlate well with high-velocity mafic rocks which crop out between the Contact fault zone and shot point 19 (Figures 2 and 16). Detailed gravity modelling suggests that the apparent dip of the Contact fault zone is approximately 45 degrees to the north in the upper layers, an interpretation which agrees with the seismic model [D. Campbell, personal communication, 1988]. Neither gravity nor seismic data, however, constrain the attitude of the fault in deeper layers.

Both gravity and magnetic values decrease northward in the dip direction, in areas corresponding to thickened sequences of flysch and steepened dip of the subducting plate (Figure 16). Along the strike profile, gravity data are difficult to interpret because the profile parallels a gravity ridge (Figure 20) [Barnes, written communication, 1988]. A relative high appears in the area of shot point 19, a trend which correlates well with the high velocities observed near that shot point. Gravity values decrease both to the east and west along the strike direction, following the trend in velocities seen in the seismic refraction data (Figure 18). Rough modelling of the gravity field to be expected for the seismic model shown in Figure 16a was done using a range of densities commonly associated with velocities indicated in the model. The results indicate that observed gravity values are well within the envelope of values generated by the model [D. Stone, written communication, 1989].

On a regional scale, there is a difference in the orientation of gravity contours from east to west of the RM1 line (Figure 20); contours to the east trend NW-SE and reflect higher negative values than those to the west, which trend SW-NE. The RM1 line is a segment of a small circle about the Euler pole which describes the relative motion between the Pacific and North American plates [Minster et al., 1974]. This line is constrained to pass through the eastern boundary of the Wadati-Benioff zone in interior Alaska [Davies, 1975; Stone, 1983]. The line corresponds to a marked change in earthquake seismicity from east to west and intersects the transect near shot
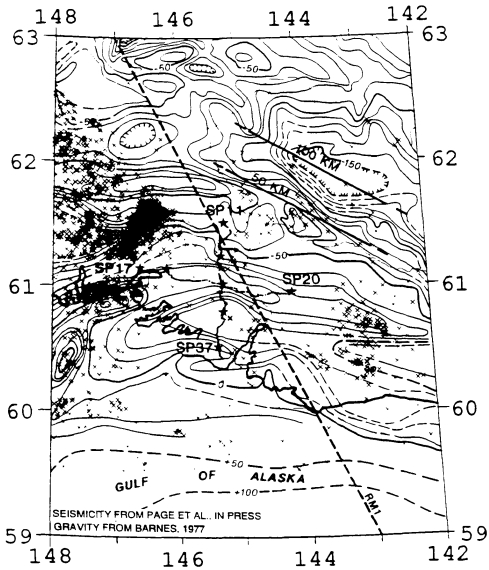
Figure 20. Regional gravity and seismicity map for southcentral Alaska. Locations shown of receivers (dotted lines) and shot points (stars). Epicenter locations are plotted for seismic events occurring below 30 km and the location of the inferred plate interface. RM1 line from Stone [1983] based on relative plate motions from the RM1 model of Minster et al. [1974]. Note change in seismicity from Aleutian Benioff to Wrangell Benioff zones on either side of the RM1 line. Inferred depth to Wrangell Benioff zone is shown by contours [Page et al., in press]. Corresponding contours of Aleutian Benioff zone are outside the area of the transect to the west and northwest.

point 12. Only epicenters for events located at 30 km or deeper are shown in the figure to reduce clutter from events in shallow layers. The majority of the events shown are thought to originate from failure in the upper portion of the subducting plate, and, if this assumption is correct, provide some indication of the depth to the lower plate in southcentral Alaska in map view. An apparent offset of Wadati-Benioff zone contours based on earthquake hypocenters occurs in the vicinity of the transect [Davies, 1975; Lahr and Plafker, 1980] and these contours roughly parallel those seen on the gravity map (Figure 20). Page et al. [in preparation] have postulated a buckle in the subducting plate as the cause of the offset. Others have suggested that a tear is responsible for the anomaly. Both the refraction and gravity data indicate that the crust of the overriding plate thickens to the north along the transect, but neither distinguishes whether a buckle rather than a tear exists in the lower plate.

Magnetic data in the offshore area also provide some insight into possible structural relationships in the lower crust. Figure 21 is a simplified map showing the magnetic lineations in the Pacific plate. These lineations are truncated by a NW-SE trending line, called the slope anomaly [Schwab et al., 1980; Bruns, 1983]. The slope anomaly has been postulated to represent a lithologic change which marks the contact of the Pacific plate with the Yakutat terrane. Based on the westward extent of the slope anomaly, it has been suggested that the Yakutat terrane extends at least as far as the transect in the subsurface [Bruns, 1983]. This westward continuation of the
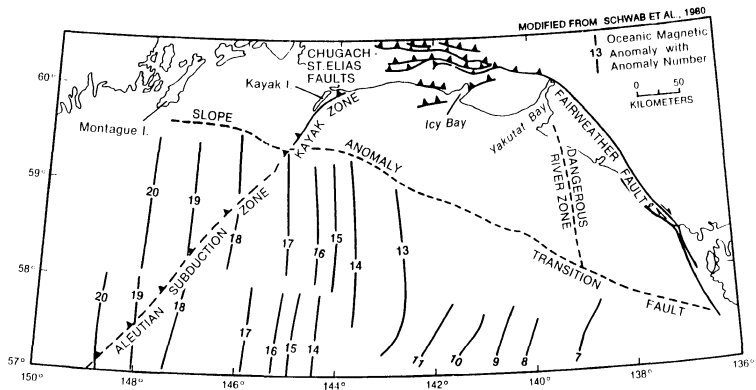
Figure 21. Map of magnetic anomalies shown in relation to major tectonic features [modified from Schwab et al., 1980; Bruns, 1983].

87

anomaly would support the correlation of the lower low-velocity zone in the seismic
model with the Yakutat terrane.

3.5.2 Rock velocity studies.

As part of the integrated effort of the TACT project, rock samples were collected
along the transect for measurements of compressional velocities. Experimental results
are described in more detail in other work [Brocher et al., 1989; Fuis et al., in
preparation]. Some of the results of studies on anisotropy in rocks of the Chugach
terrane are shown in Figure 22 [Brocher et al., 1989]. These results show that
compressional velocities in samples of Valdez Group rocks vary with the orientation of
foliation. Energy travelling parallel to the foliation direction is significantly faster than
that travelling perpendicular to foliation. In addition, the study shows that the effects
of anisotropy in the rocks can be seen to pressures of at least 600 MPa (6 kB). Figure
19 contains a comparison of primary arrival times in the records from shot point 19
along both the dip and strike profiles. Primary arrival times indicate higher average
velocities along the strike direction (approximately parallel to foliation) than along the
dip direction. From the data in Figure 19, it is difficult to determine if anisotropy
contributes to velocity variation. A meaningful comparison of primary arrivals shown
in Figure 19 for the purpose of determining anisotropy within the same rock unit
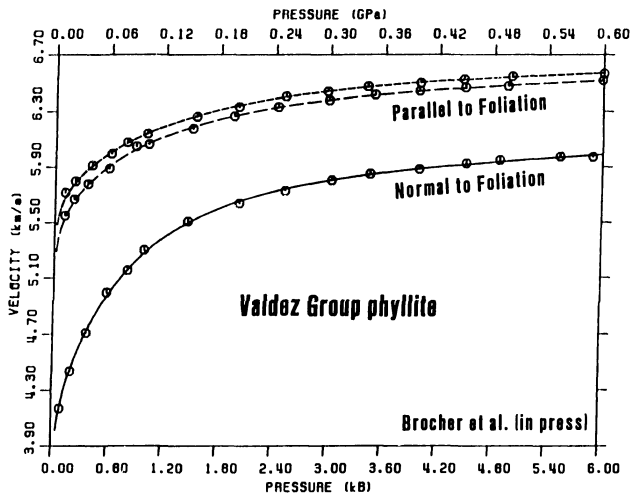cannot be carried beyond 20 km, where the energy travelling to the south crosses the

Figure 22. Laboratory measurements (made by N. Christensen) of compressional velocities in Valdez Group phyllite measured normal (solid curve) and parallel (dashed curves) to foliation [taken from Brocher et al., 1989].

89

Contact fault zone and enters the Prince William terrane. Laboratory measurements, however, indicate that anisotropy contributes to velocity variations to pressures of 600 MPa (6 kB) or approximately an 18-km depth, a finding which may account for differences between velocity-depth functions for the strike and dip directions (Figure 18).

A comparison of the velocity-depth functions from the Chugach profile with those from the Cordova Peak profile shows that velocities seen in data from the Cordova Peak line are approximately 2-4 % slower than those observed at comparable depths along the Chugach line. In the initial model, attempts to apply the velocity-depth function from the Chugach refraction data computed for the area beneath shot point 19 resulted in calculated travel times faster than those observed in the dip direction. These discrepancies can be resolved by assuming that anisotropy indicated by the difference between velocity-depth functions for the strike and dip directions results from fracture or foliation orientations, out-of-the-plane reflections, and changes in porosity and metamorphic grade.

In general, velocities in the Chugach terrane are unusually high, particularly in the region near shot point 19 (Figure 18). Direct measurements of compressional velocities of rocks sampled along the transect, although not always definitive, help to justify geologic interpretations of observed velocities. Average velocities often attributed to mafic or ultramafic oceanic rocks (6.3-7.0 km/s at 300 MPa) are observed

in metasedimentary rocks of the Valdez Group [N. Christensen, written

communication, 1988]. Average velocities at similar pressures for metavolcanic rocks,

such as pillow basalts, are even higher (6.8-7.1 km/s) [N. Christensen, written

communication, 1988]. It should be noted, however, that measurements of velocity in

different samples of a single rock type from the same location have shown variations of

up to 0.3 km/s. This degree of variability means that velocities alone cannot provide

definitive correlations with rock types. They can, however, provide some insight into

relative changes within and between units.

3.5.3 Thermal history.

Valdez Group rocks of the Chugach terrane have undergone high-

temperature/low-pressure metamorphism not easily explained by mechanisms

traditionally proposed for such regional events in subduction zone environments

[Hudson and Plafker, 1982; Sisson and Hollister, 1988]. These rocks, originally

deposited in Campanian-Maastrichtian time, were later accreted and regionally

metamorphosed. A second and more localized thermal event in Early to Middle

Eocene time resulted in metamorphism to amphibolite facies in the core of the

Chugach Metamorphic Complex. Petrologic studies of the Chugach Metamorphic

Complex indicate that temperatures during this time regionally increased near the core,

and locally increased at contacts with Eocene felsic intrusions [Hudson and Plafker, 1982].

The significance of thermal history studies for the refraction interpretation is that they provide evidence that low-pressure/high-temperature metamorphosed rocks can occur at relatively shallow depths in subduction-zone environments and that associated dewatering of sediments can produce zones of high fluid pressures and high porosities at mid-crustal depths. Studies by Sisson and others [1988; 1989] of mineralogy and CO_2-rich fluid inclusions indicate that amphibolite facies metamorphism of the rocks occurred at approximately a 10-km depth. Several mechanisms have been proposed by which the ambient temperature of the rocks could be raised to the required temperatures at such shallow depths. One such history assumes a two-stage process: massive vertical and horizontal transport of heat by fluids followed by injection of melts, both of which originate from a downdip source such as subducted young, hot oceanic crust [Hudson and Plafker, 1982; Sisson and Hollister, 1988] or a subducted spreading ridge [Marshak and Karig, 1977].

Progressive metamorphism of sedimentary rocks in a wedge and associated dewatering of sediments is seen in modern accretionary environments [Moore et al., 1987] and is thought to result in areas of high fluid pressures and high porosities. The low-velocity zones seen in the refraction data as well as the strong reflections seen in the seismic reflection data might be attributed to zones of high porosity. Areas of high

porosity have lower velocities and probably result in high impedance contrasts with surrounding areas. Dewatering of underplated sediments from subducted oceanic crust could create areas of high fluid pressures and porosity, which could in turn account for low-velocity zones in mid-crustal areas. This hypothesis has been suggested by Hyndman [1989] in his interpretation of geophysical data from offshore British Columbia. He asserts that increased porosity in crustal layers can result in velocity reductions of up to 15%, a figure which would more than adequately account for the velocity reversals seen in the southcentral Alaska data.

3.6 Discussion and summary.

An attempt to tie the model for the Chugach strike line with an interpretation of the Cordova Peak dip line to the north and south and with the mapped surface geology [Winkler and Plafker, 1981] is illustrated by the fence diagram in Figure 23. This composite diagram shows the inferred structure beneath the Chugach profile as determined from the refraction data and projects it southward based on the mapped surface geology and refraction interpretation for the Cordova Peak line. The upper layers along each refraction line have been modelled to correspond with mapped contacts between surface rocks and to reflect observed structure as far as the ray-tracing algorithm would permit.

Figure 23. Fence diagram of geologic cross sections along lines indicated in Figure 2. East-west cross section corresponds to one geologic interpretation of refraction data from the Chugach terrane. Other interpretations are discussed in the text. Connecting cross sections are based on surface geology [Winkler and Plafker, 1981]. Earthquake foci indicate approximate location of subducting plate (western line from Stephens, et al., [1984]; eastern line from Wolf et al., [1986]). The Contact fault zone (CFZ) marks the boundary of the Chugach with the Prince William terrane to the south. The terrane boundary is inferred to extend to at least 10-12 km depth. Geometry of the CFZ is not well constrained but is modelled with a moderate northward dip, consistent with geologic and gravity data [Winkler and Plafker, 1981; Page et al., 1986]. Elongate features in layer 3 (E-W panel) and layer 4A (N-S panel) correspond to high-velocity areas discussed in text. Variation in shading east of SP 19 marks the boundary of the Chugach Metamorphic Complex [Hudson and Plafker, 1982].
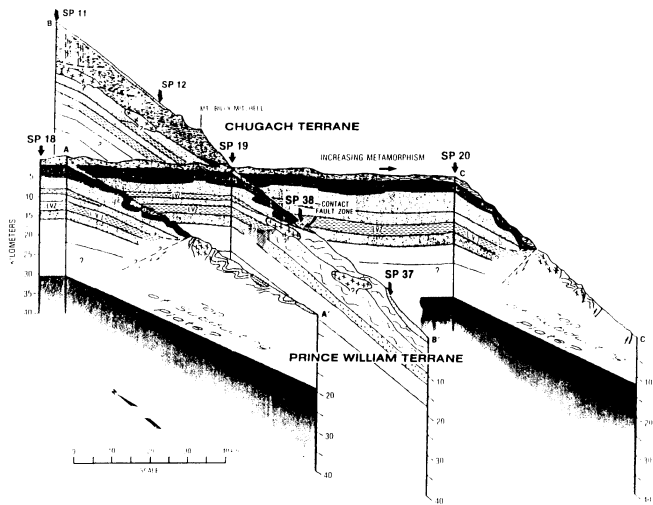
Much lateral velocity variation exists within the upper 5 km of crust in both the Chugach and Prince William terranes. In both terranes, this variation is attributed to local areas of surficial deposits, to changes in metamorphic grade and to laterally discontinuous igneous rocks which were intruded into country rock during an Eocene event. Both the Chugach and Cordova Peak refraction data contain travel time delays of energy passing through the upper layers. One possible interpretation is that these delays are the seismic expression of faults associated with the development of imbricate fans in an accretionary prism. This faulting contributes to the thickening of the upper crust, particularly in the area north of shot point 19 in the Chugach terrane.

The geometries of structures adjacent to the Contact fault system beneath layer 3A are not clear. On the surface, the Contact fault zone appears to mark a major suture which separates two geologically different rock assemblages along the transect [Winkler and Plafker, 1981]. The interpretation presented in Figures 16 and 23 is that Prince William terrane rocks have been accreted to and thrust under rocks of the Chugach terrane along the Contact fault zone. To the north of the Contact fault zone, mafic metavolcanic rocks (layer 3A) contribute to high values in gravity and magnetic data, as well as to high compressional velocities. The velocity-depth functions for the northern portion of the Cordova Peak profile indicate that these high velocities are not seen farther to the north at comparable depths. Although layer 3A is shown to pinch out near shot point 19 in the model, it may be part of an imbricated structure involving

layer 4A below. Velocities of layer 5A are similar to those in layer 2A above and may represent a downward continuation of the metamorphosed flysch. Complications in the shot record and increased velocities in the northern portion of the refraction line may be attributed to igneous intrusive rocks and fault-bounded rock units which affect the velocity structure but which are too small to model.

Mid-crustal layers beneath the Chugach terrane are assumed to be rocks which lack surface expression and do not extend southward beyond the Contact fault zone [Fuis and Ambos, 1986; Wolf and Wallace, 1988]. These lower layers have velocities compatible with those of oceanic crust, and it is suggested that they comprise layered oceanic crust that was imbricated during large-scale subduction. Velocity reversals may represent subducted sedimentary rocks which have zones of high porosity.

Model layers in the Prince William terrane correlate well with current geologic interpretation. Layers 1B-4B are correlated with sedimentary rocks which overlie rocks of the Orca Group, correlated with layers 5B and 6B. A sharp velocity contrast is observed between layers 5B and 6B, which may correspond to a compositional change between a thick sequence of interbedded sedimentary and volcanic rocks described in geologic interpretations [Winkler and Plafker, 1981; Plafker, 1987].

The velocity-depth functions of the Chugach and Prince William terranes are significantly different, particularly below a 5-km depth. Velocities in the Prince William terrane are much slower and the layer boundaries are less steeply dipping than

those of the Chugach terrane. Attempts to project layers in the upper 10 km of the Prince William terrane northward beyond the fault zone by using a reasonable velocity gradient produce calculated travel times faster than those observed in the shot records. The preferred model treats rocks of the Prince William terrane as separate geologic assemblages from those of the Chugach terrane, separated by a boundary which extends to at least a 10- to 12-km depth.

Earthquake foci are believed to delineate the top of the subducting Pacific plate at approximately a 30-km depth below the Chugach refraction line and provide a lower limit for the upper crustal package (Figure 23). Although several models exist to describe the geometry of the Wadati-Benioff zone, the refraction data do not yield much information which would better define its shape. The refraction data lack evidence of a sharp velocity contrast at the inferred location of the plate interface, a finding which suggests that the bottom of the overriding crust and the top of the subducting plate may have similar composition or physical properties. The lack of a distinct boundary at this depth may also raise the possibility that the subducting plate is actually much deeper and that earthquake events represent brittle failure in the overriding crust, or perhaps more specifically, in the subducted Yakutat terrane. Refraction data alone are insufficient to determine uniquely the complex geometries and structural relationships of the accreted Chugach, Prince William and Yakutat terranes, especially with respect to deep structure. The data do, however, provide some

constraints on the geometries, composition and structural relationships within the upper crust, particularly when synthesized with geologic and other geophysical data.

CHAPTER 4: CONCLUSIONS

The seismic model presented in this study represents an interpretation of two intersecting TACT seismic refraction profiles which are combined to yield a three-dimensional model for a part of southcentral Alaska. The model is based on a synthesis of the refraction interpretation with geologic information, potential field data and earthquake seismicity. The upper crustal velocity profile indicates unusually high velocities within the upper 10 km of crust and two mid-crustal velocity reversals. In the deeper crust, the refraction data provide evidence for a thick low-velocity zone at approximately 15-25 km depth which does not appear to extend northward beyond the Cordova Peak profile.

The refraction data from the Chugach and Cordova Peak profiles provide good restraints on crustal features which have dimensions of at least several kilometers. Faults, likely to be associated with imbricated layers in an accretionary prism, are indicated in the field data by travel time delays, loss of high frequency energy and complication from scattered or diffracted energy. At several locations, repeated or similar velocity structures provide evidence for duplicated rock assemblages. Effects of regional and local metamorphism are indicated by lateral velocity gradients within near-surface layers, where increasing velocities coincide with rocks of increasing metamorphic grade.

99

Mid-crustal low-/high-velocity layers are believed to be associated with high-amplitude secondary arrivals, en echelon travel time delays, and complication in traces on the shot records. These features are only seen when energy arriving from the shot has passed through the low-/high-velocity areas beneath the Chugach terrane. These features are not observed in the data from Prince William terrane to the south.

Distinct differences in arrival patterns and velocity-depth functions for the Prince William and Chugach terranes indicate that these two terranes represent distinct geologic rock assemblages. These differences continue to a depth of at least 10-12 km, a finding which indicates a minimum depth for the boundary between the two terranes.

The Chugach and Cordova Peak profiles offer some insight into the effects of rock anisotropy in the upper crust. Foliation orientation appears to affect observed velocities and may account for the different velocity-depth functions derived for the strike and dip directions. Although it is uncertain how deep the effects of anisotropy can be seen, the seismic model and experimental studies indicate that anisotropy may be important to depths of at least 10 km. Realization of the influence of structural properties on observed velocities in the TACT data underscores the importance of anisotropy for other crustal surveys, particularly in highly deformed areas such as fold and thrust belts and accretionary margins.

Several tectonic models have been proposed for the deep crustal structure in southcentral Alaska [e.g., Plafker et al., 1989; Lahr and Plafker, 1980; Davies, 1975;

Bruns, 1983]. The preferred model is based on the interpretation of the Chugach and Cordova Peak refraction lines and synthesized with information from geologic, seismic and potential field studies is shown in Figures 16 and 23.

Structural relationships in the geologic model indicate that the Chugach and Prince William terranes are relatively thin accretionary complexes, extending to a maximum depth of 15 km. Mid-crustal layers beneath the Chugach terrane consisting of low-/high-velocity zones are believed to pre-date accretion of the Prince William terrane, since there is no evidence that they continue south of the suture zone. Significantly different velocity-depth functions on either side of the Contact fault zone imply that the boundary between the two terranes extends to at least a 10-km depth. The best-fit seismic model in combination with geologic evidence and gravity data suggest that the Contact fault zone comprises a system of moderately to steeply north-dipping faults, at least in the upper layers. According to the seismic model, Prince William terrane rocks have been accreted and thrust beneath the mafic metavolcanic rocks which form the basement of the Chugach terrane. There is an indication from the seismic data and from geologic interpetations that one of these underthrust layers contains plutonic rocks which have been intruded into the terranes.

Travel times observed at long offsets in the shot records from the Cordova Peak line indicate the presence of a thick low-velocity layer in the lower crust. This layer is correlated with subducted continental crust of the Yakutat terrane which is currently

accreting along the Gulf of Alaska margin. The subducting Pacific plate is inferred to be beneath the Yakutat terrane in the model. Relative motion rates in the Gulf of Alaska suggest that the Yakutat terrane is moving in the same direction as the Pacific plate, but at a slightly slower rate. This discrepancy in motion can be accomodated in several ways in the model: 1) decoupling between the Pacific plate and the overriding Yakutat terrane, 2) internal deformation of the Yakutat terrane both in the Gulf and in the subsurface, and 3) strike-slip motion along inland faults. The proposed boundary of the Yakutat terrane along the dip profile correlates well with observed changes in earthquake activity on either side of the RM1 line (Figures 16 and 20). How the Yakutat terrane or, more generally, accreting continental crust, influences the stress regime, the thermal regime, the mechanical response of the plates and the pattern of earthquake occurrence are important questions which remain to be answered.

REFERENCES

Andreason, G. E., A. Grantz, I. Zietz, and D. F. Barnes, Geological interpretation of magnetic and gravity data in the Copper River Basin, Alaska, U.S. Geol. Surv. Professional Paper 316-H, pp. 135-153, 1964.

Barnes, D. F., Bouguer gravity map of Alaska, U.S. Geol. Surv. Geophysical Investigations Map GP-913, scale 1:2,500,000, 1977.

Birch, F., The velocity of compressional waves in rocks to 10 kilobars, 1, J. Geophys. Res., 65, 1083-1102, 1960.

Blundell, D. J., The Zurich 1 model: How the interpretation fared, in Workshop Proceedings, Interpretation of Seismic Wave Propagation in Laterally Heterogeneous Structure, Bureau of Mineral Resources, edited by D. M. Finlayson and J. Ansorge, Commonwealth of Australia, Report 258, 177-179, 1984, cited in G. Fuis et al., manuscript in preparation.

Brocher, T. M., M. A. Fischer, E. L. Geist and N. I. Christensen, High-resolution seismic reflection/refraction study of the Chugach-Peninsular terrane boundary, southern Alaska, J. Geophys. Res., 94, 4441-4455, 1989.

Bruns, T. R., Model for the origin of the Yakutat block, an accreting terrane in the northern Gulf of Alaska, Geology, 11, 718-721, 1983.

Cerveny, V., A. Moltokov, and I. Psencik, Ray method in Seismology, 214 pp., University of Karlova, Prague, Czechoslovakia, 1977.

Cerveny, V., and I. Psencik, SEIS83--Numerical modelling of seismic wave fields in 2-D laterally varying layered structures by the ray method, Documentation of Earthquake Algorithms, edited by E. R. Engdahl, Rep. SE-35, pp. 36-40, World Data Center (A) for Solid Earth Geophysics Boulder, Colo., 1984.

Cerveny, V., Accuracy of ray theoretical seismograms, J. Geophys., 46, 135-149, 1979.

Cerveny, V., Ray synthetic seismograms for complex two-dimensional and three-dimensional structures, J. Geophys., 58, 2-26, 1985.

Christensen, N. I., Ophiolites, seismic velocities and oceanic crustal structure, Tectonophysics, 47, 131-157, 1978.

Daley, M. A., E. L. Ambos, and G. S. Fuis, Seismic refraction data collected in the Chugach Mountains and along the Glenn Highway in southern Alaska in 1984, U.S. Geol. Surv. Open File Rep., 85-531, 32 pp., 1985.

Davies, J. N., Seismological investigations of plate tectonics in south central Alaska, Ph.D. dissertation, 193 pp., Univ. of Alaska, Fairbanks, 1975.

Dumoulin, J.A., Sandstone petrographic evidence and the Chugach-Prince William terrane boundary in southern Alaska, Geology, 16, 456-460, 1988.

Engebretson, D., A. Cox, and R. G. Gordon, Relative motions between oceanic and continental plates in the Pacific Basin, Geol. Soc. Am. Spec. Paper, 206, 54 pp., 1985.

Fischer, M. A., T. M. Brocher, W. J. Nockleberg, G. Plafker, G. L. Smith, Seismic reflection images of the crust of the northern part of the Chugach terrane, Alaska: results of a survey for the Trans-Alaska Crustal Transect (TACT), J. Geophys. Res., 94, 4424-4440, 1989.

Flueh, E., W. Mooney, G. S. Fuis, and E. L. Ambos, Crustal structure of the Chugach Mountains, southern Alaska: A study of pegleg multiples from a low-velocity zone, J. Geophys. Res., in preparation.

Fuis, G. S., and E. L. Ambos, Deep structure of the Contact Fault and the Prince William terrane: Preliminary results of the 1985 TACT seismic-refraction survey, U.S. Geological Survey Accomplishments in Alaska, 1985, U.S. Geol. Surv. Circ., 978, pp. 41-45, 1986.

Fuis, G. S., E. L. Ambos, W. D. Mooney and N. I. Christensen, Crustal structure of accreted terranes in the Chugach Mountains and Copper River Basin, southern Alaska, from seismic refraction results, J. Geophys. Res., in preparation.

Howell, D. G., D. L. Jones, and E. R. Schermer, Tectonostratigraphic terranes of the Circum-Pacific region, in, Tectonostratigraphic Terranes of the Circum-Pacific Region Earth Sci. Ser., 1, pp. 3-30, Circum-Pacific Council for Energy and Mineral Resources, Houston, Tex., 1985.

Hudson, T., and G. Plafker, Paleogene metamorphism in an accretionary flysch terrane, eastern Gulf of Alaska, Geol. Soc. Am. Bull., 92, 1280-1290, 1982.

Hyndman. R. D.. Dipping seismic reflectors, electrically conductive zones, and trapped

    water in the crust over a subducting plate, J. Geophys. Res., 93, 13,391-13,405,

    1989.

Jacob. K. H., Seismicity, tectonics, and geohazards of the Gulf of Alaska regions, in

    The Gulf of Alaska: Physical Environment and Biological Resources, edited by

    D. W. Hood and S. T. Zimmerman, OCS Study, MMS 86-0095, pp.145-184, U.S.

    Government Printing Office, Washington, D.C., 1986.

Jones, D. L., N. J. Silberling, H. C. Berg, and G. Plafker, Tectonostratigraphic terrane

    map of Alaska, U.S. Geol. Surv. Open File Rep., 81-792, 1981.

Jones, D. L., N. J. Silberling, P. J. Coney, and G. Plafker, Lithotectonic terrane map of

    Alaska (west of the 41st meridian), U.S. Geol. Surv. Misc. Field Stud. Map, MF-

    1874-A, 1987.

Lahr, J. C., Detailed seismic investigation of Pacific-North American plate interaction

    in southern Alaska, Ph.D. dissertation, 88 pp., Columbia Univ., New York, 1975.

Lahr, J. C., and G. Plafker, Holocene Pacific-North American plate interaction in

    southern Alaska: implications for the Yakataga seismic gap, Geology, 8, 483-486,

    1980.

Luetgert, J., Programs RAY86 and R86PLT: Interactive two-dimensional

    raytracing/synthetic seismogram package (VAX/VMS) version, U.S. Geol. Surv.,

    Menlo Park, Calif., 1987.

Ma, C., J. W. Ryan, and D. Caprette, Crustal dynamics project data analysis--1988. VLBI geodetic results 1979-87, NASA Technical Memorandum 100723, 214 pp., 1989.

Marshak, R.S., and D. E. Karig, Triple junctions as a cause for anomalously near-trench igneous activity between the trench and volcanic arc, Geology, 5, 233-236, 1977.

Meissner, R., The continental crust: A geophysical approach, 426 pp., Academic Press, Inc., Florida, 1986.

Minster, J. B., T. J. Jordan, P. Molnar, and E. Haines, Numerical modelling of instantaneous plate tectonics, Royal Astron. Soc., Geophys. J., 36, 541, 1974.

Minster, J. B. and T. H. Jordan, Present day plate motions, J. Geophys. Res., 83, 5331-5354, 1978.

Moore, J.C., A. Mascle, E. Taylor, and ODP Leg 110 Scientific Staff, Expulsion of fluids from depth along a subduction-zone decollement horizon, Nature, 326, 785-788, 1987.

Nokleberg, W. J., G. Plafker, J. S. Lull, W. K. Wallace, and G. R. Winkler, Structural analysis of the southern Peninsular, southern Wrangellia, and northern Chugach terranes along the Trans-Alaska Crustal Transect, northern Chugach Mountains, Alaska, J.Geophys. Res., 94, 4297-4320, 1989.

Page, R. A., G. Plafker, G. S. Fuis, W. J. Nokleberg, E. L. Ambos, W. E. Mooney, and D. L. Campbell, Accretion and subduction tectonics in the Chugach Mountains and Copper River Basin, Alaska: Initial results of the Trans-Alaska Crustal Transect, Geology, 14, 501-505, 1986.

Page, R. A., C. D. Stephens, and J. C. Lahr, Seismicity of the Wrangell-Benioff zones and the North American plate along the Trans-Alaska Crustal Transect, Chugach Mountains and Copper River Basin, southern Alaska, J. Geophys. Res., in preparation.

Panuska, B. C., and D. B. Stone, Latitudinal motion of the Wrangellia and Alexander terranes and the southern Alaska superterrane, in Tectonostratigraphic Terranes of the Circum-Pacific Region Earth Sci. Ser., 1, edited by D. G. Howell, pp., 109-120, Circum-Pacific Council for Energy and Mineral Resources, Houston, Tex., 1985.

Perez O. J., and K. H. Jacob, Tectonic model and seismic potential of the eastern Gulf of Alaska and Yakataga seismic gap, J. Geophys. Res., 85, 7132-7150, 1980.

Plafker, G., W. J. Nokleberg, J. S. Lull, S. M. Roeske and G. R. Winkler, Nature and timing of deformation along the Contact Fault System in the Cordova, Bering Glacier and Valdez Quadrangle, U.S. Geological Survey Accomplishments in Alaska, 1985, U.S. Geol. Surv. Circ., 978, 74-77, 1986.

Plafker, G., Regional geology and petroleum potential of the northern Gulf of Alaska
    continental margin, in Geology and Resource Potential of the Continental Margin
    of Western North America and Adjacent Ocean Basins, AAPG Circum-Pac. Earth
    Sci. Ser. 6, edited by D. W. Scholl, A. Grantz, and J. G. Vedder, pp.229-268,
    American Association of Petroleum Geologists, Houston, Tex., 1987.

Plafker, G., W. J. Nokleberg and J. S. Lull, Bedrock geology and tectonic evolution of
    the Wrangellia, Peninsular, and Chugach terranes along the Trans-Alaska Crustal
    Transect in the Chugach Mountains and southern Copper River Basin, J.
    Geophys. Res., 94, 4255-4295, 1989.

Plumley, P. W., and G. Plafker, Additional estimate of paleolatitude for
    Paleocene/Eocene? Prince William terrane--Orca volcanics (abstract) Alaska,
    Tectonics, 2, 295-314, 1983.

Rau, W. W., G. Plafker, and G.R. Winkler, Foraminiferal stratigraphy and correlations
    in the Gulf of Alaska Tertiary province, U.S. Geol. Surv. Oil Gas Invest. Chart,
    OC-120, 1983.

Salisbury, M. H., and N. I. Christensen, The seismic velocity structure of a traverse
    through the Bay of Islands ophiolite complex, Newfoundland, an exposure of
    oceanic crust and upper mantle, J. Geophys. Res., 83, 805-817, 1978.

Schwab. W. C., T. R. Bruns, and R. von Huene. Maps showing structural interpretation of magnetic lineaments in the northern Gulf of Alaska, scale 1:1,500,00, U.S. Geol. Surv. Misc. Field Stud. Map, MF-1245, 1980.

Silberling, N. J., and D. L. Jones, Lithotectonic terrane maps of the North American Cordillera, U.S. Geol. Surv. Open File Rep., 84-523, A1-A12, 1984.

Sisson, V. B., and L. S. Hollister, Low-pressure facies series metamorphism in an accretionary sedimentary prism, southern Alaska, Geology, 16, 358-361, 1988.

Sisson, V. B., L. S. Hollister, and T. C. Onstott, Petrologic and age constraints on the origin of a low-pressure/high-temperature metamorphic complex, southern Alaska, J. Geophys. Res., 94, 4392-4410, 1989.

Spudich, P., and J. Orcutt, Petrology and porosity of an oceanic crustal site: Results from wave form modeling of seismic refraction data, J. Geophys. Res., 85, 1409-1433, 1980.

Stephens, C. D., K. A. Fogelman, J. C. Lahr, and R. A. Page, Wrangell Benioff zone, southern Alaska, Geology, 12, 373-376, 1984.

Stone, D. B., and B. C. Panuska, Paleolatitudes versus time for southern Alaska, J. Geophys. Res., 87, 3697-3707, 1982.

Stone, D. B., Present day plate boundaries in Alaska and the Arctic, in Proceedings Symposium, Western Alaska Geology and Resource Potential, 3, Anchorage, 1-14, 1983.

Stone D. B., R. A. Page, and J. N. Davies, (ed.), Trans-Alaska lithospheric
investigation--program prospectus, U.S. Geol. Surv. Circ., 984, 24 pp., 1986.

Stone, D. B. and W. K. Wallace, A geologic framework of Alaska, Episodes, 10, 283-
289, 1987.

Turner, F. J., Metamorphic petrology, McGraw-Hill Book Co., Inc., New York, 1981.

U.S. Geological Survey, Aeromagnetic map of parts of the Cordova and Middleton
Island 1 by 3 degree quadrangles, Alaska, scale 1:250,000, U.S. Geol. Surv. Open
File Report 79-223, 1979a.

_____, Aeromagnetic map of part of the Valdez 1 by 3 degree quadrangle, Alaska, U.S.
Geol. Surv. Open File Report 79-381, 1979b.

Vidale, J., Finite-difference calculation of travel times, Bull. Seis. Soc. Am., 78, 2062-
2076, 1988.

von Huene, R., G. Keller, T. R. Bruns, and K. McDougall, Cenozoic migration of
Alaskan terranes indicated by paleontologic study, in Tectonostratigraphic
Terranes of the Circum-Pacific Region, Earth Sci. Ser., 1, edited by D. G. Howell,
pp. 121-136, Circum-Pacific Council for Energy and Mineral Resources, Houston,
Tex., 1985.

Wallace, W. K., Structure and petrology of a portion of a regional thrust zone in the
central Chugach Mountains, Alaska, Ph.D. dissertation, 254 pp., Univ. of Wash.,
Seattle, 1981.

Wallace, W. K., Deformation and metamorphism in a convergent margin setting, northern Chugach Mountains, Alaska, <u>Geol. Soc. Am. Abstr. Programs</u>, <u>16</u>, 339, 1984.

Wallace, W. K., Tectonic evolution of the Haley Creek terrane, a rootless thrust sheet in the Chugach Mountains, Alaska, <u>Geol. Soc. Am. Abstr. Programs</u>, <u>17</u>, 416, 1985.

Wilson, J. M., P. Meador and G. Fuis, Data report for the 1985 TACT seismic refraction survey, south-central Alaska, <u>U.S. Geol. Surv. Open File Rep.</u>, <u>87-440</u>, 78 pp., 1987.

Winkler, G. R., and G. Plafker, Geologic map and cross sections of the Cordova and Middleton Island quadrangles, southern Alaska, scale 1:250,000, <u>U.S. Geol. Surv. Open File Rep.</u>, <u>81-1164</u>, 26 pp., 1 sheet, 1981.

Winkler, G. R., M. L. Silberman, A. Grantz, R. J. Miller, and E. M. MacKevett, Jr., Geologic map and summary geochronology of the Valdez quadrangle, southern Alaska, scale 1:250,000, <u>U.S. Geol. Surv. Open File Rep.</u>, <u>80-892A</u>, 2 sheets, 1981.

Wolf, L. W., A. R. Levander, and G. Fuis, Upper crustal structure of the accreted Chugach terrane, Alaska, <u>Eos Trans. AGU</u>, <u>67</u>, 44, 1195, 1986.

Wolf, L. W., and W. K. Wallace, Upper crustal structure of the Chugach and Prince William terranes, Alaska, <u>Eos Trans. AGU</u>, <u>69</u>, 44, 1988.

Wolf, L. W. and A. R. Levander, Upper crustal structure of the accreted Chugach terrane, Alaska, J. Geophys. Res., 94, 4457-4466, 1989.

APPENDIX

Methodology.

Data analysis of the Chugach and Cordova Peak seismic refraction lines followed a systematic procedure commonly used in interpreting refraction data. Particulars of the experiment, such as shot sizes, receiver locations, etc., were obtained from the data reports [Daley et al., 1985; Wilson et al., 1987]. Data from both profiles were made available by the U.S. Geological Survey for the purpose of interpretation. Software was provided by Cerveny and Psencik (SEIS83) [1984] and by Luetgert (RAY86 and R86PLT) [1987]. Trace-normalized shot records were produced and compared with true-amplitude records. Differences between the two were minimal and because trace-normalized record sections are easier to view, they were used in the analysis and for illustration.

The first stage in developing a starting model for use in the ray tracing programs was to synthesize information from the shot records with geologic information. The procedure was as follows:

1) Primary and secondary arrivals were determined from shot records, which were plotted at a reducing velocity of 6 km/s. This reduction velocity was chosen because it represents an average crustal velocity and therefore

allows deviations from the average to be recognized more easily. Arrival times were picked from a video monitor. The program used automatically adjusts the pick to the nearest seismic trace [Luetgert, 1987]. This method reduces error in determining offset distances and allows for a subjective determination of arrival times.

2)   Once primary arrival times were determined, a one-dimensional model for each shotpoint was derived based on apparent velocities and intercept times of the main refractors.

3)   One-dimensional models were then combined for adjacent shotpoints to produce a two-dimensional model. Contacts on published geologic maps were correlated with locations along the profile and average values for dips of contacts and bedding were incorporated into model layers. The model was then parameterized for use in the raytracing programs, SEIS83 [Cerveny and Psencik, 1984] and RAY86 [Luetgert, 1987] and iteratively adjusted to match calculated travel times of primary and secondary arrivals with those of the observed data.

4)   The two-dimensional models were expanded to include shotpoints at progressively farther offset distances to image deeper structure, once satisfactory matches to near offsets were acheived. In short, development of the model proceeded from the surface downward.

5) Once most calculated travel times were fit to within 0.05-0.10 s of observed arrivals, synthetic seismograms were generated to match phases and to model amplitudes.

Computational programs.

Both raytracing programs used in the analysis are based on a ray series solution to the equation of motion. This solution is a high-frequency approximation, and as such, can only be applied to smooth media in which the characteristic dimensions of inhomogeneities are much larger than the prevailing wavelength of the propagating wave. The predominant frequency of the TACT data was approximately 10 Hz. SEIS83 uses the method of two-point raytracing with a modified shooting method. Given a starting angle, the program iteratively "shoots" rays through an angle sweep until an endpoint (or receiver location) is reached. RAY86 uses initial value raytracing and interpolates between nearest endpoints for information at a specific receiver location. Hence the RAY86 program is faster but less precise.

Once first-arriving energy on the shot record is matched, critical points are adjusted by shifting between sharp vertical velocity discontinuities to transition zones or by changing gradients. Velocities versus depths can also be manipulated. For shallow structure, there is a "trade off" between velocity and depth to a particular layer. That is, to match arrivals for near offsets, a boundary can be raised or lowered, or

alternatively, the velocity can be slowed or increased. As offsets increase, however, travel times become less sensitive to changes in depth than to corresponding changes in velocities. Amplitude information and other waveform characteristics provide some constraint on the structure at this point in the modeling process.

Ray synthetics from SEIS83 (SYNPLT) are based only on real-valued solutions from dynamic raytracing. Details of this method can be found in Cerveny [1985]. Essentially, five real-valued wave quantities (the real travel time and two real-valued numbers for the two components of displacement) are calculated and stored with endpoint information. Elementary wave quantities are summed and, for a specified receiver location, are interpolated between stored endpoints. In R86PLT [Luetgert, 1987], complex-valued amplitudes are calculated and a geometric spreading factor is applied. Phase and amplitude information are then convolved with a source-time function to produce the synthetic seismogram.

Accuracy of ray methods.

Amplitude information generated by ray methods provides constraints on the velocity structure. There are, however, certain limitations of the method because it is approximate. Ray methods are not reliable in shadow zones, for complex structures (e.g., pinch-outs, fault zones, etc.) or for near-critical arrivals. Exact methods, such as finite differencing and reflectivity, are more useful for modelling diffractions, arrivals

from complex structure, and multiples because they more completely describe the wave field.

The best-fit model presented in the text is non-unique. Where identification of phases is straightforward, wide-angle reflections give good estimates of depths to interfaces [Meissner, 1986]. Mismatches on the order of a few tens of milliseconds yield estimated depth errors of no more than several hundred meters, if an average crustal velocity of 6.0 km/s is assumed. Additional uncertainties are encountered in low-velocity zones, where a trade-off exists between velocity and depth to the interface. Depths to these boundaries are estimated to be accurate to about 10%. Where available, reflection data has been used to provide a constraint on the depths to interfaces.

An additional example of non-uniqueness of solution is in the choice between using a velocity discontinuity (or interface) or a steep velocity gradient. Amplitude information can be used to assist in making this choice. Steeper gradients cause the rays to diverge more rapidly, resulting in smaller amplitudes. Amplitudes also change with respect to angle of incidence, and therefore can be used model interface locations [Meissner, 1986]. Rays travelling closest to the critical angle and to the turning angle produce the greatest amplitudes. Matching relative amplitudes of secondary-arriving energy can refine impedance contrasts to within a few percent for individual interfaces within the model.

On the basis of amplitude information, the best-fit model represents the closest overall match to travel times and phases identified in the refraction data. Other models may be equally plausible. Because of the associated uncertainties in the refraction modelling, rationales for the geometry of layers for each profile are discussed in the sections entitled "Data and analysis." Further constraints on the model provided by geologic and other geophysical data sets are discussed in separate sections following the data analysis.

Despite the limitations of ray methods as a forward modelling technique, reassurance of its validity and a feeling for its accuracy can be found in comparisons with exact methods such as finite-differencing and reflectivity [Cerveny, 1979; Cerveny, 1985; Vidale, 1988]. Given that major phases in the data are properly identified, the configuration of velocity contours will not change upon re-analysis [Blundell, 1984].